Quantification of the Hydrophobic Effect Using Water-Soluble Super Aryl-Extended Calix[4]pyrroles

L. Escobar[a,b] and P. Ballester[a,c,*]

E-mail: *pballester@iciq.es

[a] Institute of Chemical Research of Catalonia (ICIQ), The Barcelona Institute of Science and Technology (BIST), Av. Països Catalans, 16, 43007, Tarragona, Spain.
[b] Universitat Rovira i Virgili, Departament de Química Analítica i Química Orgànica, c/Marcel·lí Domingo, 1, 43007, Tarragona, Spain.
[c] ICREA, Passeig Lluís Companys, 23, 08010, Barcelona, Spain.

Supporting Information

1. General information and instruments

Reagents were obtained from commercial suppliers and used without further purification unless otherwise stated. All solvents were commercially obtained and used without further purification excess pyrrole that was distilled and freshly used. Dry solvents were taken from a solvent system MB SPS 800 or obtained after drying with appropriate desiccants. Routine ^{1}H NMR and $^{13}C\{^{1}H\}$ NMR spectra were recorded on a Bruker Avance 300 (300 MHz for ^{1}H NMR and 75 MHz for ^{13}C NMR), Bruker Avance 400 (400 MHz for ^{1}H NMR and 100 MHz for ^{13}C NMR), Bruker Avance 500 (500 MHz for ^{1}H NMR and 125 MHz for ^{13}C NMR) or Bruker Avance 500 with cryoprobe (500 MHz for ^{1}H NMR and 125 MHz for ^{13}C NMR). Deuterated solvents used are indicated in the characterization and chemical shifts are given in ppm. Residual solvent peaks were used as reference.[1] All NMR *J* values are given in Hz. COSY, NOESY, HMQC and HMBC were recorded to help with the assignment of ^{1}H and ^{13}C signals. High Resolution Mass Spectra (HRMS) were obtained on a Bruker HPLC-TOF (MicroTOF Focus) with ESI as ionization mode and Bruker HPLC-QqTOF (MaXis Impact) with ESI as ionization mode. IR spectra were recorded on a Bruker Optics FTIR Alpha spectrometer equipped with a DTGS detector, KBr beam splitter at 4 cm^{-1} resolution using a one bounce ATR accessory with diamond windows. Melting points were measured on a MP70 Melting Point System Mettler Toledo instrument. ITC titrations were carried out on a Microcal VP-ITC MicroCalorimeter. Column chromatography purifications were performed with silica gel technical grade (Sigma-Aldrich), pore size 60 Å, 230-400 mesh particle size, 40-63 μm particle size and Thin Layer Chromatography (TLC) analyses on silica gel 60 F254.

2. Synthesis and characterization data

2.1 Tetra-(4-iodophenyl) calix[4]pyrrole 1a

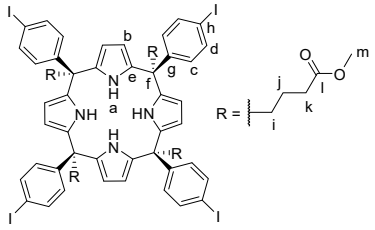

Figure S1. Line-drawing structure of *αααα*-**1a**.

A solution of methyl 5-(4'-iodophenyl)-5-oxopentanoate **2a** (1 g, 3.01 mmol, 1 equiv.) in CH_2Cl_2 (10 mL) was stirred under Argon atmosphere and protected from the light by covering the flask with foil. Then, 37% HCl (0.51 mL, 6.02 mmol, 2 equiv.) was added dropwise over 5 min. Finally, distilled pyrrole (0.25 mL, 3.61 mmol, 1.2 equiv.) was added dropwise over 5 min. The mixture was stirred at r.t. under Argon atmosphere for 72 h. After that, the crude was concentrated, redissolved in CH_2Cl_2 (10 mL) and washed with $NaHCO_3$ (aq. sat.) (2x10 mL) and water (10 mL). The organic layer was dried (Na_2SO_4), filtered and concentrated to dryness. The crude was purified by column chromatography on silica gel (50 g, 80:19:1 CH_2Cl_2:Hexane:MTBE) affording *αααα*-**1a** as a white solid. Compound *αααα*-**1a** was recrystallized from 3:2 CH_3OH:CH_2Cl_2 (108 mg, 0.07 mmol, 10% yield). Rf = 0.20 (80:19:1 CH_2Cl_2:Hexane:MTBE). ^{1}H NMR (400 MHz, $CDCl_3$, 298 K): *δ* (ppm) = 8.01 (br s, 4H); 7.53-7.51 (m, 8H); 6.95-6.93 (m, 8H); 5.81 (s, 8H); 3.62 (s, 12H); 2.29 (m, 16H); 1.59 (m, 8H). ^{13}C{^{1}H} NMR (125 MHz, $CDCl_3$, 298 K): *δ* (ppm) = 174.4; 145.4; 136.5; 135.2; 130.9; 106.7; 92.4; 51.7; 49.1; 38.4; 33.4; 20.3. HRMS (ESI-TOF) m/z: $[M-H]^-$ Calcd for $C_{64}H_{63}I_4N_4O_8$ 1523.0830; Found 1523.0835. FTIR $\overline{\nu}$ (cm^{-1}) = 3393; 2920; 1731; 1572; 1482; 1434; 1259; 1169; 1004; 770; 723; 507. M.p > 130ºC (decompose).

Other calix[4]pyrrole isomers of **1a** were isolated from the crude. Compounds *ααα**β***-**1a** and *αα**ββ***-**1a** were isolated in 5% and 3% yields, respectively. Characterization for *ααα**β***-**1a**: Rf = 0.30 (80:19:1 CH_2Cl_2:Hexane:MTBE). ^{1}H NMR (400 MHz, $CDCl_3$, 298 K): *δ* (ppm) = 7.82 (br s, 2H); 7.63-7.61 (m, 2H); 7.55-7.52 (m, 6H); 7.21-7.19 (m, 2H); 6.93-6.88 (m, 6H); 5.92 (dd, *J* = 2.4 Hz; *J* = 2.4 Hz, 2H); 5.87 (dd, *J* = 2.4 Hz; *J* = 2.4 Hz, 2H); 5.83 (dd, *J* = 2.4 Hz; *J* = 2.4 Hz, 2H); 5.81 (dd, *J* = 2.4 Hz; *J* = 2.4 Hz, 2H); 3.64 (s, 3H); 3.62 (s, 9H); 2.34-2.14 (m, 16H); 1.57-1.33 (m, 8H). ^{13}C{^{1}H} NMR (125 MHz, $CDCl_3$, 298 K): *δ* (ppm) = 173.9; 173.8; 144.8; 137.4; 136.8; 136.8; 135.3; 135.0; 134.8; 134.5; 130.7; 130.6; 130.4; 107.0; 106.8; 106.6; 106.3; 92.5; 51.7; 49.0; 48.8; 34.0; 33.6; 20.5. HRMS (ESI-TOF) m/z: $[M+Na]^+$ Calcd for $C_{64}H_{64}I_4N_4O_8Na$ 1547.0795; Found 1547.0774. FTIR $\overline{\nu}$ (cm^{-1}) = 3396; 2947; 1734; 1483; 1413; 1565; 1170; 1145; 1005; 770; 726; 511. M.p > 125ºC (decompose). Characterization for *αα**ββ***-**1a**: Rf = 0.60 (80:19:1 CH_2Cl_2:Hexane:MTBE). ^{1}H NMR (400 MHz, $CDCl_3$, 298 K): *δ* (ppm) = 7.56 (br s, 2H); 7.53-7.51 (m, 8H); 7.30 (br s, 2H); 6.93-6.91 (m, 8H); 5.89 (d, *J* = 2.4 Hz, 4H); 5.86 (d, *J* = 2.4 Hz, 4H); 3.64 (s, 12H); 2.34-2.08 (m, 16H); 1.50-1.46 (m, 8H). ^{13}C{^{1}H} NMR (125 MHz, $CDCl_3$, 298 K): *δ* (ppm) = 174.0; 144.3; 137.1; 135.3; 134.4; 130.3; 106.8; 106.5; 51.7; 48.9; 33.8; 20.5. HRMS (ESI-TOF) m/z: $[M+Na]^+$ Calcd for $C_{64}H_{64}I_4N_4O_8Na$ 1547.0795; Found 1547.0778. FTIR $\overline{\nu}$ (cm^{-1}) = 2963; 1734; 1570; 1483; 1413; 1260; 1146; 1002; 769; 729; 662; 512. M.p > 120ºC (decompose).

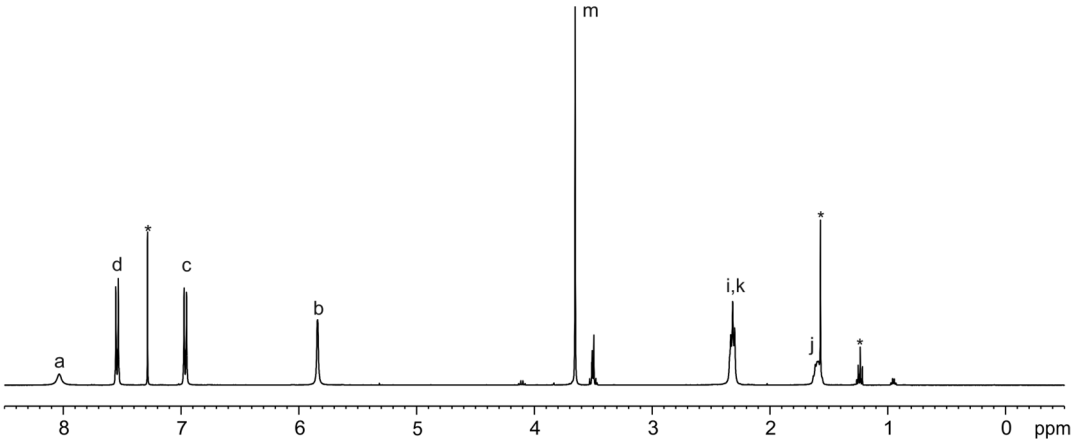

Figure S2. ^{1}H NMR (400 MHz, $CDCl_3$, 298 K) spectrum of *αααα*-**1a**. See Figure S1 for proton assignment. *Solvent residual peaks.

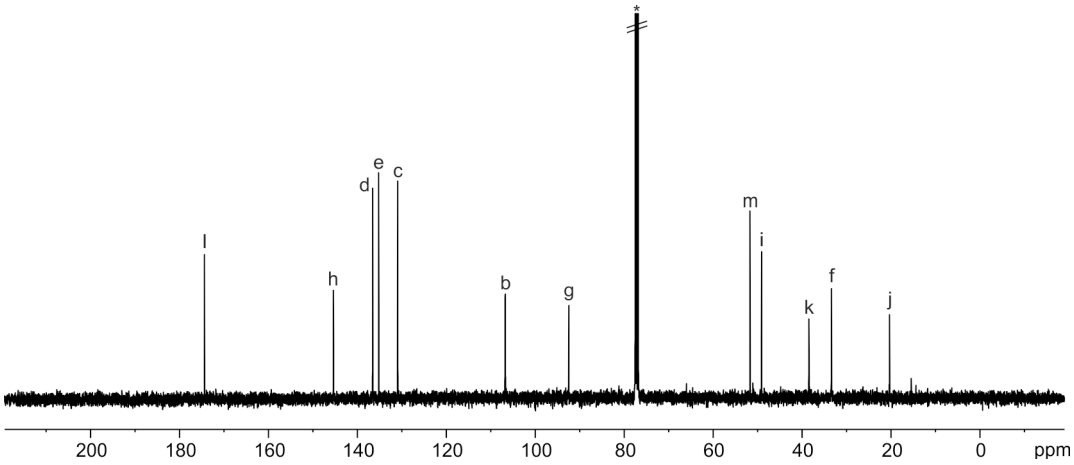

Figure S3. $^{13}C\{^{1}H\}$ NMR (125 MHz, $CDCl_3$, 298 K) spectrum of *αααα*-**1a**. See Figure S1 for proton assignment. *Solvent residual peak.

Reaction conditions for the synthesis of tetra-(4-iodophenyl) calix[4]pyrrole **1a**:

Table S1. Conditions for the synthesis of **1a**:

Entry	Acid (equiv.)	Additive[a] (equiv.)	Solvent (0.3-0.5 M)	Time (h)	Result (% yield)[c]
1	4 M HCl in dioxane (2)	-	CH_2Cl_2	72	**2a** and oligomers
2	4 M HCl in dioxane (2)	3	CH_2Cl_2	72	**2a** and oligomers
3	CH_3SO_3H (2/2)[b]	-	CH_3OH/CH_2Cl_2	24/48	*ααββ*- (10) and *αααβ*-**1a** (10)
4	37% HCl (2)	-	CH_2Cl_2	72	*ααββ*- (3), *αααβ*- (5) and *αααα*-**1a** (10)
5	37% HCl (2)	3	CH_2Cl_2	72	**2a** and oligomers

[a] Tricaprylmethylammonium chloride (mixture C_8-C_{10}; C_8 is dominant) or methyltributylammonium chloride. [b] Reaction performed in two steps: Reaction using 1) CH_3SO_3H in CH_3OH for 24 h and 2) CH_3SO_3H in CH_2Cl_2 for 48 h. [c] Reaction crudes were analysed by ^{1}H NMR spectroscopy and yields are given for isolated compounds.

Reaction crude from the synthesis of **1a** using 37% HCl (entry 5, Table S1) was analyzed by HPLC (method: Spherisorb silica gel column (80 Å, 5 μm, 4.6 mm x 250 mm); 97.5:2.5 CH_2Cl_2:MTBE; flux = 1 mL/min; injections of 10 μL; detection at 250 nm, 240 nm and 235 nm).

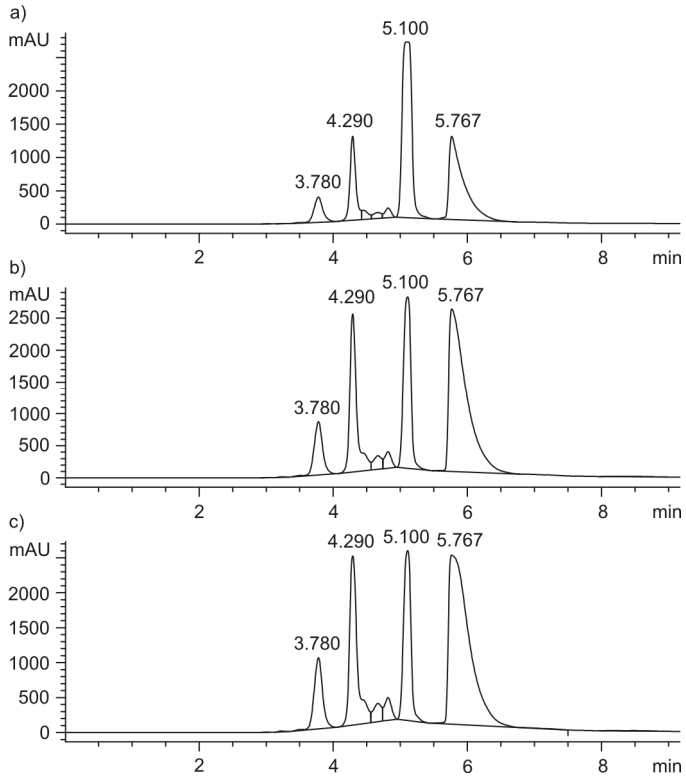

Figure S4. Chromatograms of the reaction crude (10 mg/mL solution) using different detection wavelengths: a) 250 nm; b) 240 nm and c) 235 nm.

Table S2. Results obtained from Figure S4:

Peak	Retention time (min)	Relative area	Compound
1	3.78	1	*ααββ*-**1a**
2	4.29	2	*αααβ*-**1a**
3	5.10	5.5	**2a**
4	5.77	4	*αααα*-**1a**

2.2 Tetra-(4-iodophenyl) calix[4]pyrrole 1b

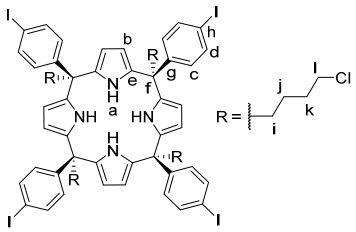

Figure S5. Line-drawing structure of *αααα*-**1b**.

Compound *αααα*-**1b** was synthetized following a methodology previously described by our research group.[2] 4-Iodophenyl 4'-chlorobutyl ketone **2b** (1 g, 3.10 mmol, 1 equiv.) and methyltributylammonium chloride (2.19 g, 9.30 mmol, 3 equiv.) were dissolved in dry CH_2Cl_2 (6.2 mL). The mixture was stirred at r.t. under Argon atmosphere and pyrrole (0.22 mL, 3.10 mmol, 1 equiv.) was added dropwise. HCl (2.33 mL from a 4 M solution in dioxane, 9.30 mmol, 3 equiv.) was added dropwise. The flask was covered with foil and stirred for 72 hours. After that, the crude was diluted with CH_2Cl_2 (50 mL) and washed with $NaHCO_3$ (aq. sat.) (2x50 mL) and water (50 mL). The organic layer was dried (Na_2SO_4), filtered and concentrated. The crude was suspended in 4:6 CH_2Cl_2:Hexane, filtered and purified by column chromatography on silica gel (80 g, 4:6 CH_2Cl_2:Hexane). The product was further purified by recrystallization from 1:1 CH_2Cl_2:CH_3OH affording *αααα*-**1b** as a white solid (119 mg, 0.08 mmol, 10%). Rf = 0.3 (4:6 CH_2Cl_2:Hexane). ^{1}H NMR (400 MHz, $CDCl_3$, 298 K): δ (ppm) = 7.54-7.52 (m, 8H); 7.27 (br s, 4H); 6.85-6.83 (m, 8H); 5.84 (s, 8H); 3.49 (t, J = 6.0 Hz, 8H); 2.24 (m, 8H); 1.73 (m, 8H); 1.34 (m, 8H). ^{13}C{^{1}H} NMR (100 MHz, $CDCl_3$, 298 K): δ (ppm) = 144.3; 137.0; 135.2; 130.4; 106.8; 92.6; 48.8; 44.8; 39.5; 32.9; 22.8. HRMS (ESI-TOF) m/z: $[M+H]^+$ Calcd for $C_{60}H_{61}Cl_4I_4N_4$ 1484.9824; Found 1484.9780. FTIR $\overline{\nu}$ (cm^{-1}) = 2948; 2867; 1567; 1483; 1416; 1390; 1306; 1187; 1046; 1004; 768. M.p. > 110ºC (decompose).

Other calix[4]pyrrole isomers of **1b** were isolated from the crude. A mixture of *ααaβ*-**1b** and *ααββ*-**1b** was isolated in a total 30% yield.

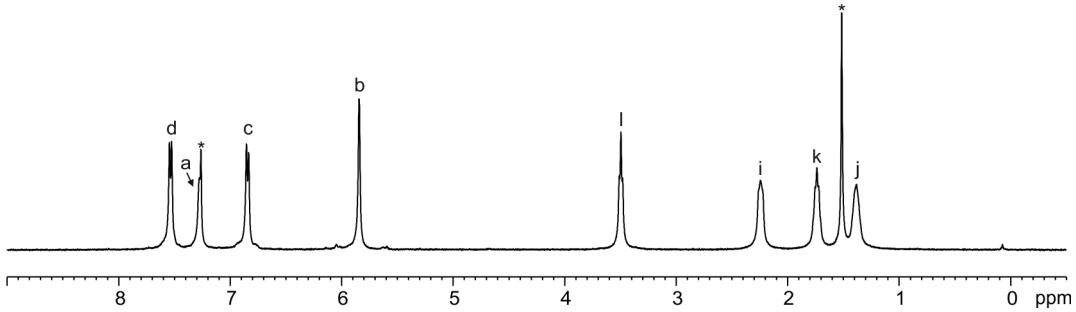

Figure S6. ^{1}H NMR (400 MHz, $CDCl_3$, 298 K) spectrum of *αααα*-**1b**. See Figure S5 for proton assignment. *Solvent residual peaks.

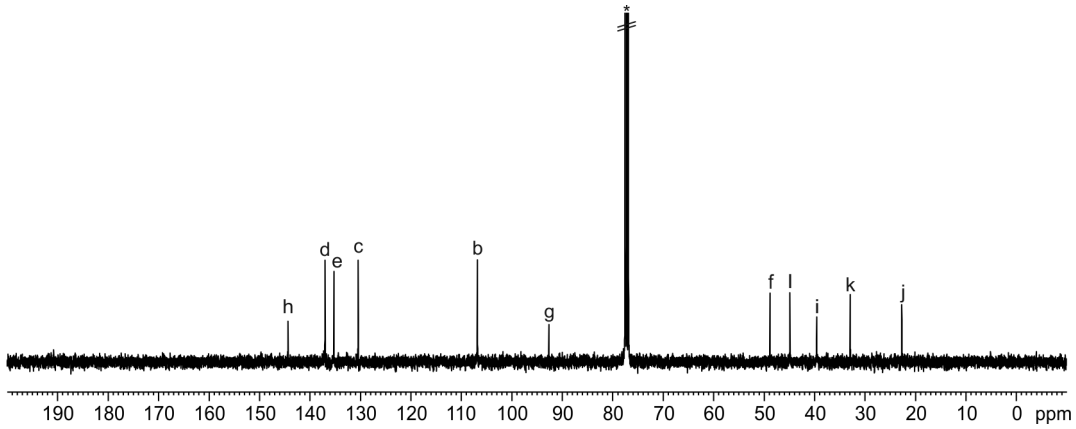

Figure S7. $^{13}C\{^{1}H\}$ NMR (125 MHz, $CDCl_3$, 298 K) spectrum of *αααα*-**1b**. See Figure S5 for proton assignment. *Solvent residual peak.

2.3 5-(4'-Iodophenyl)-5-oxopentanoate 2a

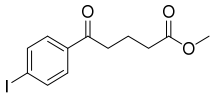

Figure S8. Line-drawing structure of **2a**.

5-(4'-Iodophenyl)-5-oxopentanoate **2a** was prepared following a described procedure in literature.[2]

2.4 4-Iodophenyl 4'-chlorobutyl ketone 2b

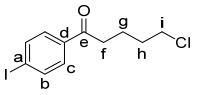

Figure S9. Line-drawing structure of **2b**.

Compound **2b** was synthetized following a similar procedure described in literature.[3,4] Part 1. Magnesium turnings (0.46 g, 18.76 mmol, 1 equiv.) were added to an oven-dried round bottomed flask and purged with Argon. Dry THF (2 mL) was added and the mixture was sonicated for 10 min. Then, the flask was connected to an addition funnel and it was slowly stirred under Argon atmosphere. 1-Chloro-4-bromo butane (2.16 mL, 18.76 mmol, 1 equiv.) was added to the addition funnel and diluted with dry THF (12 mL). The 1-chloro-4-bromo butane solution was added dropwise to the magnesium for 1 hour. The temperature was controlled with an ice bath. After the addition, dry THF (4 mL) was added to the addition funnel and added dropwise to the reaction. The reaction was stirred at r.t. for 30 minutes and the magnesium was totally consumed. Part 2. 4-Iodobenzoyl chloride (5 g, 18.76 mmol, 1 equiv.), $Fe(acac)_3$ (0.33 g, 0.94 mmol, 0.05 equiv.) and dry THF (13 mL) were added to an oven-dried round bottomed flask. The mixture was stirred under Argon atmosphere and cooled at -78ºC. The freshly prepared Grignard reagent was added dropwise for 5 min. The reaction flask was covered with foil. THF (4 mL) was added to the flask of the Grignard reagent and added to the reaction. The reaction was stirred at -78ºC for 1 h and at r.t. for 23 h. After that, the reaction was stopped and water (30 mL) was added. The crude was extracted with CH_2Cl_2 (3x30 mL) and the organic layer was washed with 1 N HCl (30 mL) and water (2x30 mL). The organic layer was dried, filtered (Na_2SO_4) and concentrated. A mixture of 4:6 CH_2Cl_2:Hexane was added to the crude and filtered. The crude was purified by column chromatography on silica gel (400 g, 4:6 CH_2Cl_2:Hexane) affording the product as white solid (1.51 g, 4.69 mmol, 25%). Rf = 0.2 (4:6 CH_2Cl_2:Hexane). ^{1}H NMR (400 MHz, $CDCl_3$, 298 K): δ (ppm) = 7.84-7.82 (m, 2H); 7.67-7.65 (m, 2H); 3.58 (t, J = 6.2 Hz, 2H); 2.97 (t, J = 6.8 Hz, 2H); 1.88 (m, 4H). $^{13}C\{^{1}H\}$ NMR (100 MHz, $CDCl_3$, 298 K): δ (ppm) = 199.0; 138.1; 136.2; 129.6; 101.1; 44.8; 37.6; 32.1; 21.5. HRMS (ESI-TOF) m/z: $[M+Na]^+$ Calcd for $C_{11}H_{12}ClOINa$ 344.9514; Found 344.9514. FTIR $\overline{\nu}$ (cm^{-1}) = 2943; 2898; 1689; 1581; 1560; 1467; 1390; 1293; 1178; 1058; 1005; 974. M.p. = 74-75ºC.

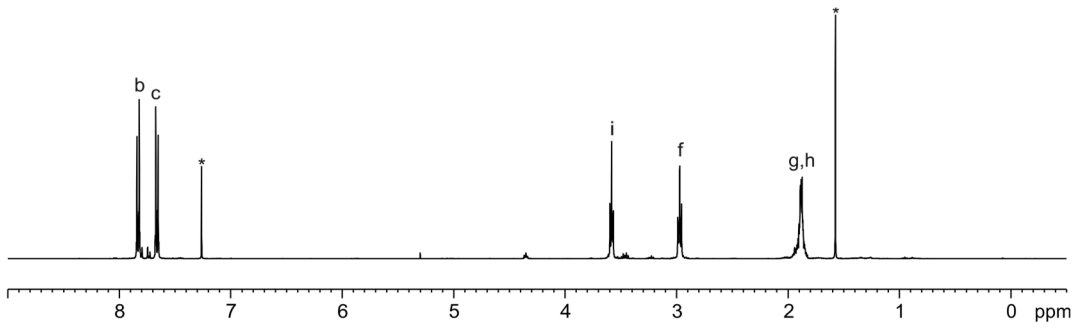

Figure S10. ^{1}H NMR (400 MHz, $CDCl_3$, 298 K) spectrum of **2b**. See Figure S9 for proton assignment. *Solvent residual peaks.

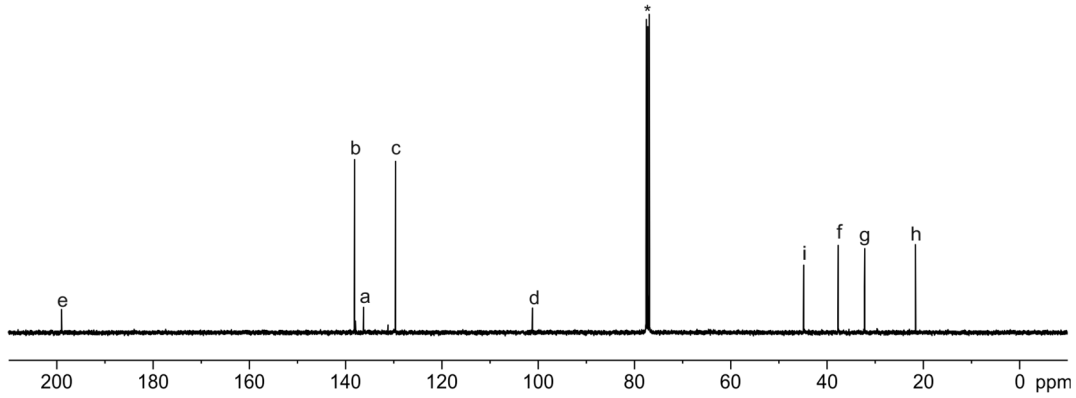

Figure S11. $^{13}C\{^{1}H\}$ NMR (125 MHz, $CDCl_3$, 298 K) spectrum of **2b**. See Figure S9 for proton assignment. *Solvent residual peak.

2.5 Methyl (4-ethynylphenoxy)acetate 3a

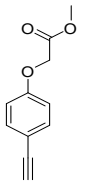

Figure S12. Line-drawing structure of **3a**.

Methyl (4-ethynylphenoxy)acetate **3a** was prepared following a procedure previously described in literature.[5,6,7]

2.6 (1-Chlorobutyloxy-4-ethynyl)benzene 3b

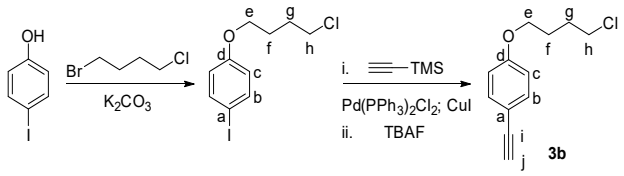

Scheme S1. Synthesis of (1-chlorobutyloxy-4-ethynyl)benzene **3b**.

1-(4'-Chlorobutoxy)-4-iodobenzene: 4-Iodophenol (0.5 g, 2.27 mmol, 1 equiv.) was dissolved in dry DMF (50 mL) and stirred at r.t. under Argon atmosphere. K_2CO_3 (0.47 g, 3.41 mmol, 1.5 equiv.) was added and the reaction was stirred for 2 h. 1-Bromo-4-chlorobutane (0.31 mL, 2.73 mmol, 1.2 equiv.) was added and the reaction was stirred for 22 h. After that, the reaction was stopped and 1 N HCl was added until pH = 5. The compound was extracted by adding CH_2Cl_2 and water (4x15 mL of CH_2Cl_2 and 4x15 mL of water). The organic layer was washed with water (3x50 mL), dried (Na_2SO_4), filtered and concentrated. The crude was purified by silica gel column chromatography (20 g, 3:7 CH_2Cl_2:Hexane) affording the product as a colorless oil (0.47 g, 1.51 mmol, 66%). Rf = 0.5 (3:7 CH_2Cl_2:Hexane). ^{1}H NMR (300 MHz, $CDCl_3$, 298 K): δ (ppm) = 7.56-7.53 (m, 2H); 6.68-6.65 (m, 2H); 3.96 (t, J = 5.6 Hz, 2H); 3.61 (t, J = 6.1 Hz, 2H); 1.98-1.93 (m, 4H). $^{13}C\{^{1}H\}$ NMR (75 MHz, $CDCl_3$, 298 K): δ (ppm) = 158.9; 138.4; 117.0; 82.9; 67.2; 44.8; 29.4; 26.7. HRMS (ESI-TOF) m/z: $[M]^{+}$ Calcd for

$C_{10}H_{12}ClOI$ 309.9616; Found 309.9621. FTIR $\overline{\nu}$ (cm^{-1}) = 2955; 2873; 1585; 1572; 1485; 1469; 1441; 1280; 1239; 1174; 1100; 1049.

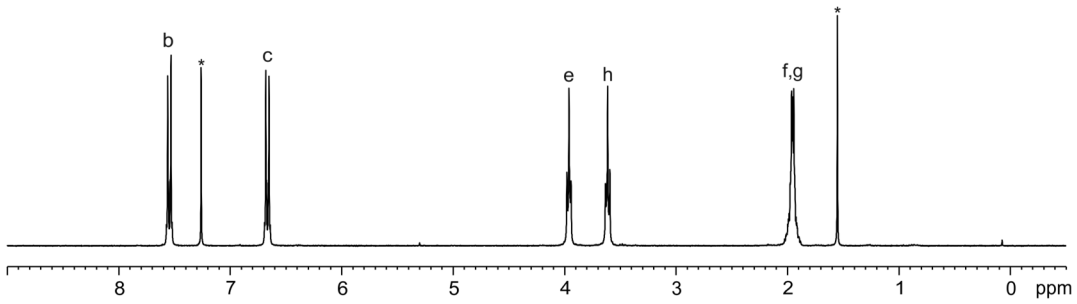

Figure S13. ^{1}H NMR (300 MHz, $CDCl_3$, 298 K) spectrum of 1-(4'-chlorobutoxy)-4-iodobenzene. See Scheme S1 for proton assignment. *Solvent residual peaks.

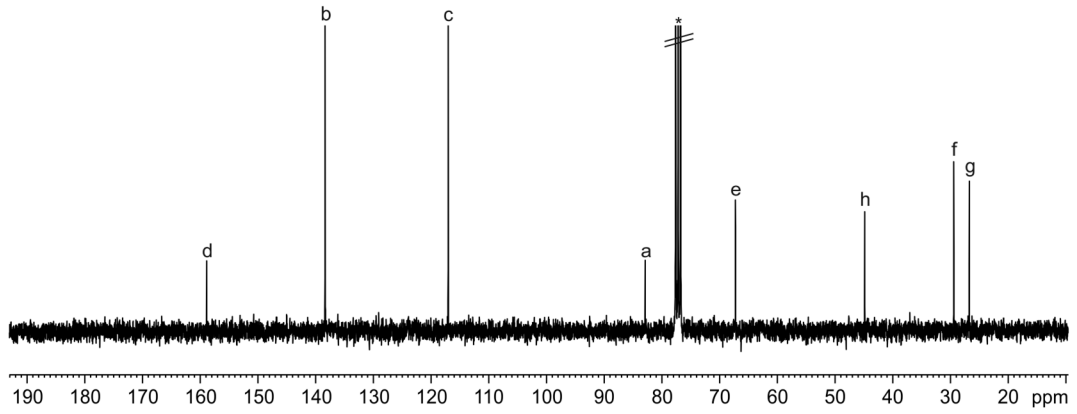

Figure S14. $^{13}C\{^{1}H\}$ NMR (75 MHz, $CDCl_3$, 298 K) spectrum of 1-(4'-chlorobutoxy)-4-iodobenzene. See Scheme S1 for proton assignment. *Solvent residual peak.

(1-Chlorobutyloxy-4-ethynyl)benzene 3b: Step i. 1-(4'-Chlorobutoxy)-4-iodobenzene (1 g, 3.22 mmol, 1 equiv.), $Pd(PPh_3)_2Cl_2$ (170 mg, 0.24 mmol, 0.07 equiv.) and CuI (170 mg, 0.90 mmol, 0.28 equiv.) were kept under Argon atmosphere. Dry and degassed THF (32 mL) and DIPEA (1.68 mL, 9.66 mmol, 3 equiv.) were added. Ethynyltrimethylsilane (1.37 mL, 9.66 mmol, 3 equiv.) was added. The reaction was stirred at 45ºC for 3 h. After that, the reaction was stopped and the crude was concentrated. The crude was redissolved in CH_2Cl_2 (50 mL) and washed with 1 N HCl (50 mL), brine (50 mL) and water (50 mL). The organic layer was dried (Na_2SO_4), filtered and concentrated. The crude was suspended in 2:8 CH_2Cl_2:Hexane, filtered and purified by column chromatography on silica gel (20 g, 2:8 CH_2Cl_2:Hexane). The protected alkyne was isolated as an orange oil (697 mg, 2.48 mmol, 77%). Step ii. The protected alkyne (697 mg, 2.48 mmol, 1 equiv.) was dissolved in THF (20 mL). TBAF (2.73 mL, 2.73 mmol, 1.1 equiv.) was added dropwise. The reaction was stirred at r.t. under Argon atmosphere for 15 min. After that, the reaction was quenched with NH_4Cl (20 mL). EtOAc (20 mL) and water (20 mL) were added. THF was removed under vacuum. The crude was extracted with EtOAc (3x20 mL) and the organic layer was washed with brine (20 mL), dried (Na_2SO_4), filtered and concentrated. The crude was suspended in 2:8 CH_2Cl_2:Hexane, filtered and purified by silica gel column chromatography (8 g, 2:8 CH_2Cl_2:Hexane). The product was isolated as a pale yellow solid (284 mg, 1.36 mmol, 55%). Rf = 0.3 (2:8 CH_2Cl_2:Hexane). ^{1}H NMR (400 MHz, $CDCl_3$, 298 K): δ (ppm) = 7.43-7.41 (m, 2H); 6.84-6.82 (m, 2H); 4.00 (t, J = 5.8 Hz, 2H); 3.62 (t, J = 6.1 Hz, 2H); 2.99 (s, 1H); 1.99-1.94 (m, 4H). $^{13}C\{^{1}H\}$ NMR (100 MHz, $CDCl_3$, 298 K): δ (ppm) = 159.4; 133.8; 114.6; 114.4; 83.8; 75.9; 67.2; 44.8; 29.4; 26.7. HRMS (ESI-TOF) m/z: $[M+H]^+$ Calcd for $C_{12}H_{14}ClO$ 209.0728; Found 209.0723. FTIR $\overline{\nu}$ (cm^{-1}) = 2960; 2939; 2906; 2869; 2100; 1604; 1505; 1398; 1293; 1247; 1174; 1034. M.p. = 53-55ºC.

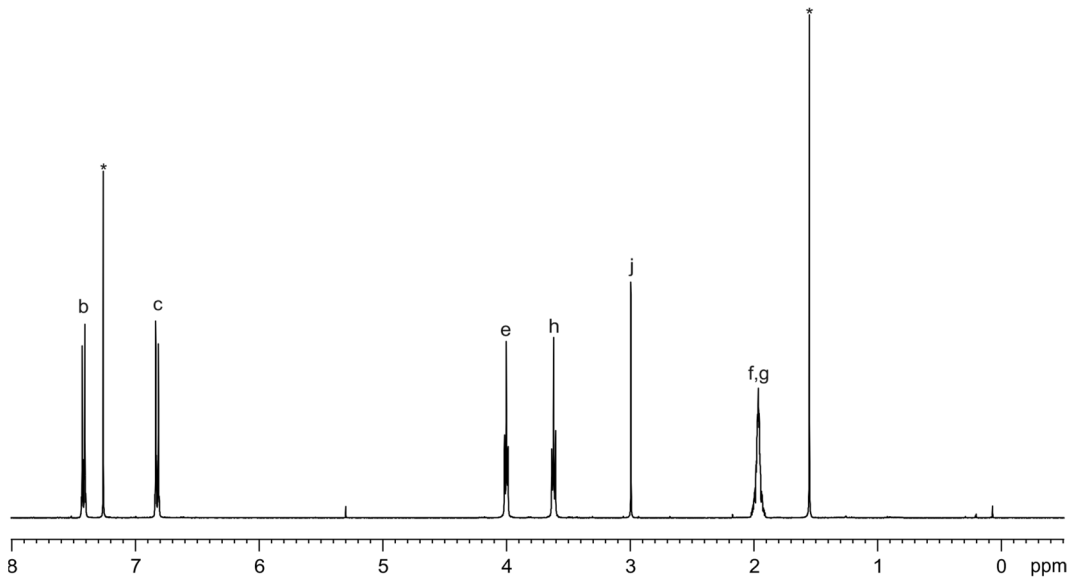

Figure S15. ^{1}H NMR (400 MHz, $CDCl_3$, 298 K) spectrum of **3b**. See Scheme S1 for proton assignment. *Solvent residual peaks.

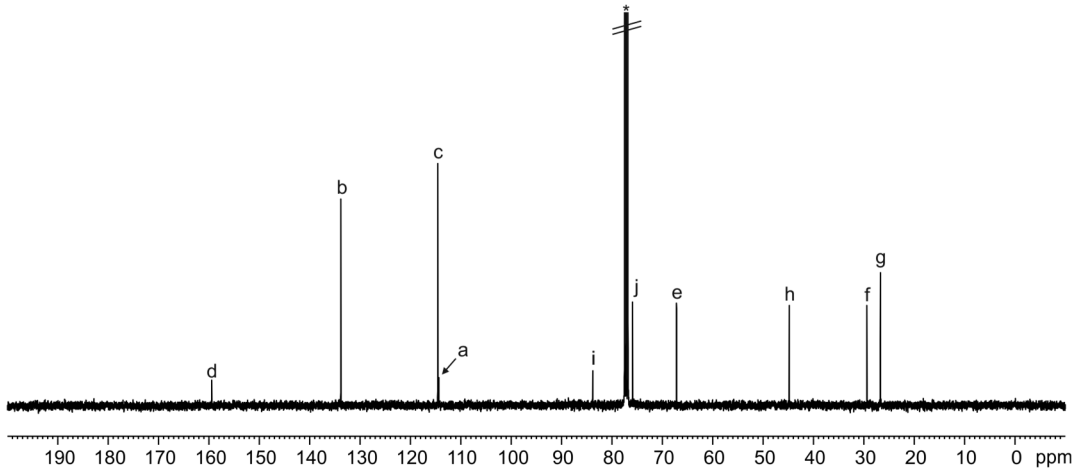

Figure S16. $^{13}C\{^{1}H\}$ NMR (100 MHz, $CDCl_3$, 298 K) spectrum of **3b**. See Scheme S1 for proton assignment. *Solvent residual peak.

2.7 Octa-ester super aryl-extended calix[4]pyrrole 4a

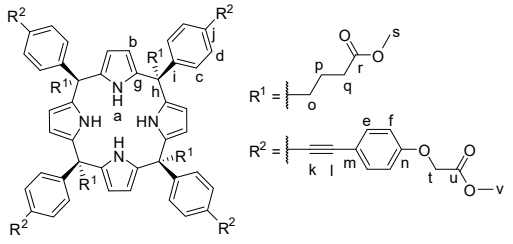

Figure S17. Line-drawing structure of **4a**.

Compound *αααα*-**1a** (50 mg, 0.03 mmol, 1 equiv.), $Pd(PPh_3)_2Cl_2$ (2.88 mg, 0.004 mmol, 0.03 equiv.), CuI (1.25 mg, 0.007 mmol, 0.05 equiv.) and methyl (4-ethynylphenoxy)acetate **3a** (37.40 mg, 0.20 mmol, 1.50 equiv.) were dissolved in dry THF (5 mL). The mixture was stirred under Argon atmosphere and dry diisopropylamine (5 mL) was added. The reaction was stirred at 45ºC for 5 h. After that, the reaction was stopped and the crude was concentrated. The crude was redissolved in CH_2Cl_2 (10 mL) and washed with 0.05 N HCl (10 mL), brine (10 mL) and water (10 mL). The organic layer was dried (Na_2SO_4), filtered and concentrated. The crude was purified by column chromatography on silica gel (6 g silica gel, 98:2 → 95:5 CH_2Cl_2:MTBE) affording the product as a white solid. The product was recrystallized from 3:1 CH_3OH:Et_2O (38.40 mg, 0.02 mmol, 70% yield). Rf = 0.25 (98:2 CH_2Cl_2:MTBE). ^{1}H NMR (400 MHz, $CDCl_3$, 298 K): δ (ppm) = 8.01 (br s, 4H); 7.47-7.45 (m, 8H); 7.37-7.35 (m, 8H); 7.20-7.18 (m, 8H); 6.87-6.85 (m, 8H); 5.86 (s, 8H); 4.65 (s, 8H); 3.81 (s, 12H); 3.64 (s, 12H); 2.36-2.32 (m,

8H); 2.31 (dd, *J* = 6.6 Hz, *J* = 6.6 Hz, 8H); 1.63-1.59 (m, 8H). $^{13}C\{^{1}H\}$ NMR (100 MHz, $CDCl_3$, 298 K): *δ* (ppm) = 174.4; 169.2; 157.8; 145.6; 135.4; 133.3; 130.7; 128.8; 121.7; 117.0; 114.8; 106.7; 89.0; 88.6; 65.4; 52.5; 51.7; 49.3; 38.6; 33.6; 20.5. HRMS (ESI-TOF) m/z: $[M+Na]^+$ Calcd for $C_{108}H_{100}N_4O_{20}Na$ 1795.6823; Found 1795.6824. FTIR $\overline{\nu}$ (cm^{-1}) = 3368; 2951; 1733; 1513; 1435; 1284; 1203; 1174; 1076; 830; 773; 538. M.p > 185ºC (decompose).

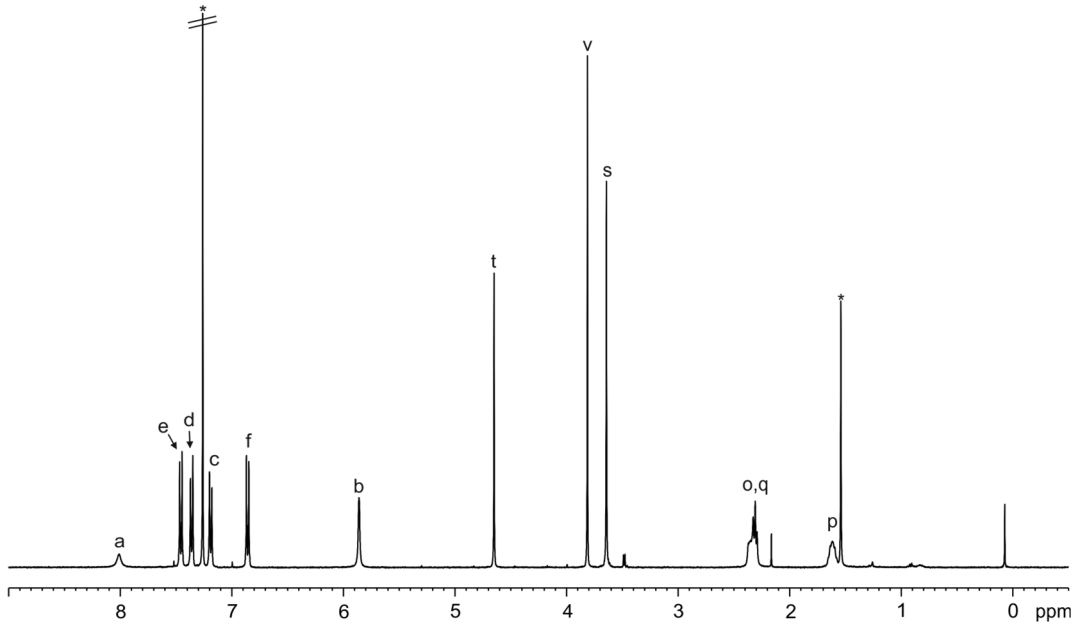

Figure S18. ^{1}H NMR (400 MHz, $CDCl_3$, 298 K) spectrum of **4a**. See Figure S17 for proton assignment. *Solvent residual peaks.

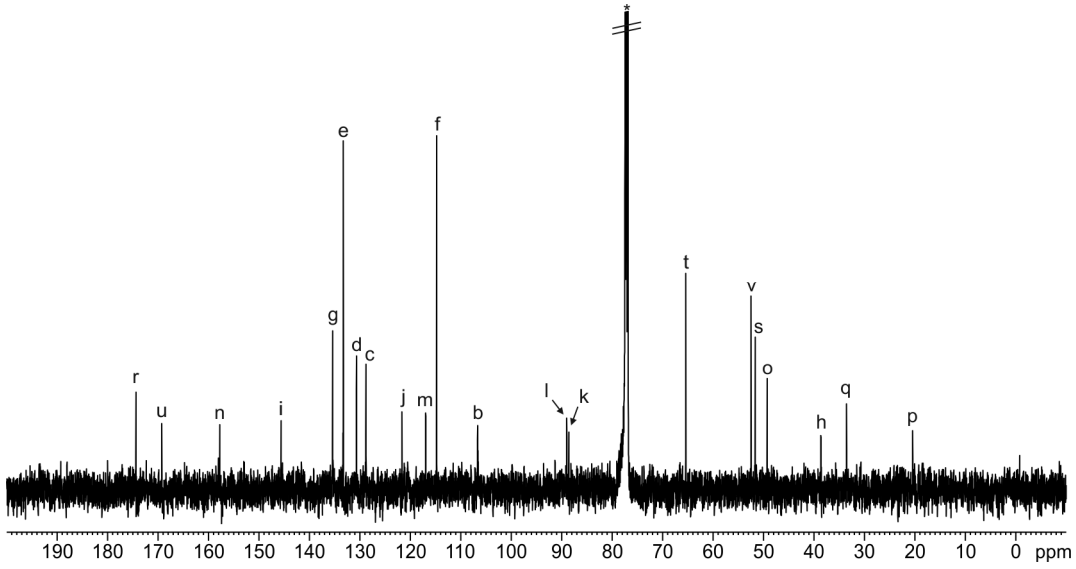

Figure S19. $^{13}C\{^{1}H\}$ NMR (100 MHz, $CDCl_3$, 298 K) spectrum of **4a**. See Figure S17 for proton assignment. *Solvent residual peak.

2.8 Octa-chloro super aryl-extended calix[4]pyrrole 4b

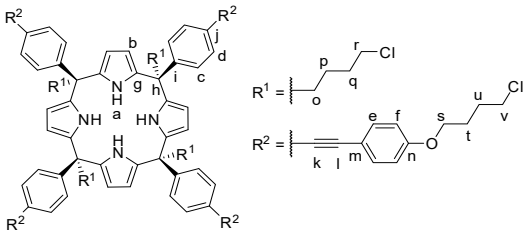

Figure S20. Line-drawing structure of **4b**.

Compound *αααα*-**1b** (52 mg, 0.035 mmol, 1 equiv.), (1-chlorobutyloxy-4-ethynyl)benzene **3b** (43.40 mg, 0.208 mmol, 1.5 equiv.), $Pd(PPh_3)_2Cl_2$ (3.07 mg, 0.004 mmol, 0.03 equiv.) and CuI (1.33 mg, 0.007 mmol, 0.05 equiv.) were kept under Argon atmosphere. Dry and degassed THF (5 mL) and diisopropylamine (5 mL) were added. The reaction was stirred at 45ºC for 3.5 h. After that, the reaction was stopped and the crude was concentrated. The crude was redissolved in CH_2Cl_2 (10 mL) and washed with 0.5 N HCl (10 mL), brine (10 mL) and water (10 mL). The organic layer was dried (Na_2SO_4), filtered and concentrated. The crude was purified by column chromatography on silica gel (6 g, 1:1 → 8:2 CH_2Cl_2:Hexane, the crude was adsorbed on silica gel) affording the product as white solid. The product was sonicated in CH_3CN (3 mL) and washed with extra CH_3CN (2 mL) (37.98 mg, 0.021 mmol, 60%). Rf = 0.6 (8:2 CH_2Cl_2:Hexane). ^{1}H NMR (400 MHz, $CDCl_3$, 298 K): *δ* (ppm) = 7.44-7.42 (m, 8H); 7.40 (br s, 4H); 7.39-7.37 (m, 8H); 7.10-7.08 (m, 8H); 6.82-6.80 (m, 8H); 5.88 (d, *J* = 2.2 Hz, 8H); 4.00 (t, *J* = 5.5 Hz, 8H); 3.63 (t, *J* = 6.0 Hz, 8H); 3.50 (t, *J* = 6.6 Hz, 8H); 2.32-2.28 (m, 8H); 2.00-1.94 (m, 16H); 1.79-1.72 (m, 8H); 1.45-1.37 (m, 8H). ^{13}C{^{1}H} NMR (100 MHz, $CDCl_3$, 298 K): *δ* (ppm) = 159.0; 144.5; 135.5; 133.3; 131.0; 128.3; 122.1; 115.6; 114.6; 106.6; 89.7; 88.0; 67.2; 48.9; 44.9; 44.8; 39.6; 33.1; 29.4; 26.8; 22.7. MS (MALDI-TOF) m/z: $[M]^{\cdot+}$ Calcd for $C_{108}H_{108}Cl_8N_4O_4$ 1804.6; Found 1804.4. $[M+H]^+$ Calcd for $C_{108}H_{109}Cl_8N_4O_4$ 1805.6; Found 1805.4. $[M-C_4H_8Cl]^{\cdot+}$ Calcd for $C_{104}H_{100}Cl_7N_4O_4$ 1713.6; Found 1713.4. FTIR $\overline{\nu}$ (cm^{-1}) = 2952; 2871; 1607; 1569; 1515; 1473; 1286; 1253; 1174; 1050; 1030; 833. M.p. > 205 ºC (decompose).

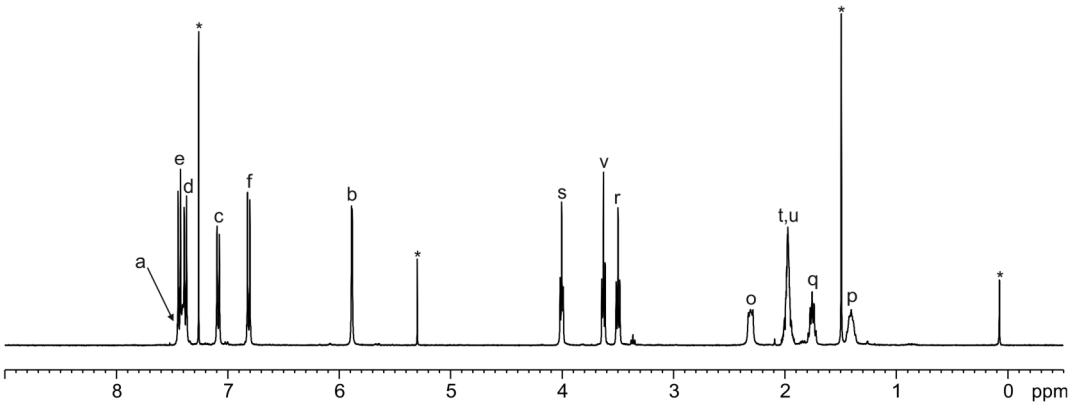

Figure S21. ^{1}H NMR (400 MHz, $CDCl_3$, 298 K) spectrum of **4b**. See Figure S20 for proton assignment. *Solvent residual peaks.

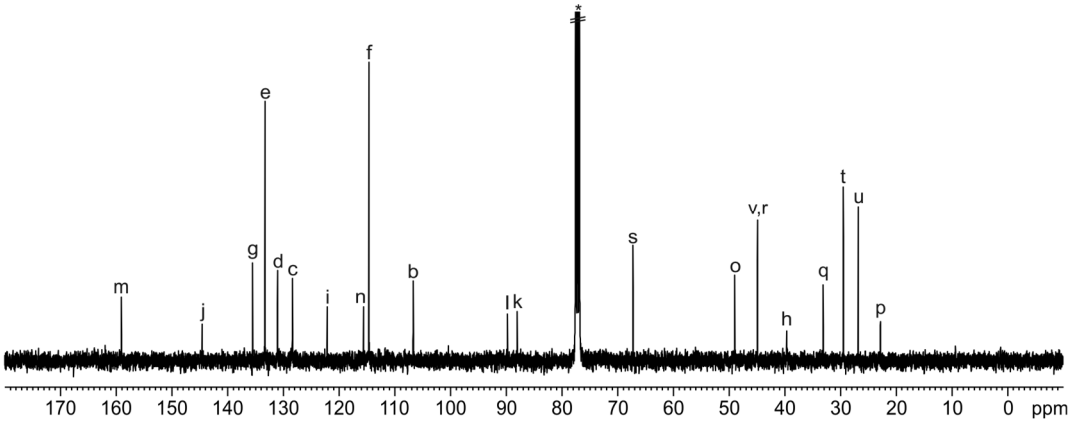

Figure S22. ^{13}C{^{1}H} NMR (100 MHz, $CDCl_3$, 298 K) spectrum of **4b**. See Figure S20 for proton assignment. *Solvent residual peak.

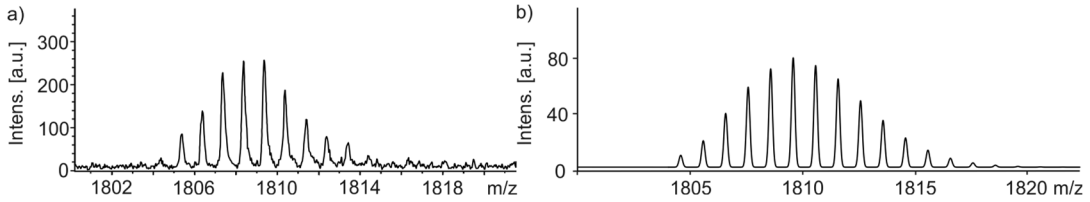

Figure S23. Experimental (a) and theoretical (b) isotopic distributions of the mixture of ions $[M]^{\cdot+}$ and $[M+H]^{+}$ of **4b**.

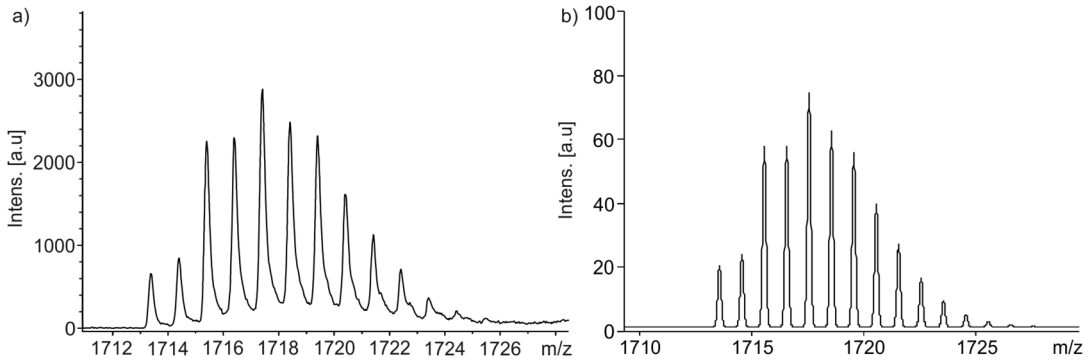

Figure S24. Experimental (a) and theoretical (b) isotopic distributions of the ion $[M\text{-}C_4H_8Cl]^{\cdot+}$ of **4b**.

2.9 Octa-acid super aryl-extended calix[4]pyrrole 5

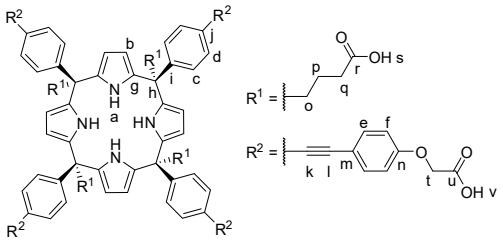

Figure S25. Line-drawing structure of **5**.

Octa-ester calix[4]pyrrole **4a** (38 mg, 0.02 mmol, 1 equiv.) was dissolved in THF (10 mL). LiOH (8.21 mg, 0.34 mmol, 2 equiv.) was dissolved in water (3 mL) and added to the previous solution. The reaction was stirred at 40ºC for 24 h. After that, the reaction was stopped and the organic solvent was evaporated under reduced pressure. Additional water (7 mL) was added to the crude and the aqueous layer was washed with CH_2Cl_2 (10 mL). Then, the aqueous layer was acidified with 1 N HCl until pH = 3 and the white precipitate was extracted with EtOAc (3x10 mL). The organic layer was dried (Na_2SO_4), filtered and concentrated affording the product as a white solid (34 mg, 0.02 mmol, 96% yield). ^{1}H NMR (400 MHz, $(CD_3)_2CO$, 298 K): δ (ppm) = 8.44 (br s, 4H); 7.51-7.49 (m, 8H); 7.39-7.36 (m, 8H); 7.08-7.06 (m, 8H); 6.90-6.88 (m, 8H); 6.10 (d, J = 2.4 Hz, 8H); 4.78 (s, 8H); 2.48-2.44 (m, 8H); 2.28 (dd, J = 7.2 Hz, J = 7.2 Hz, 8H); 1.45-1.41 (m, 8H). ^{13}C{^{1}H} NMR (100 MHz, $(CD_3)_2CO$, 298 K): δ (ppm) = 174.6; 170.4; 159.3; 147.2; 137.6; 133.8; 131.9; 130.0; 122.8; 116.6; 115.8; 106.5; 90.3; 88.4; 65.5; 49.3; 40.6; 34.2; 21.5. HRMS (ESI-TOF) m/z: $[M\text{-}3H]^{3-}$ Calcd for $C_{100}H_{81}N_4O_{20}$ 552.5154; Found 552.5176. FTIR $\overline{\nu}$ (cm^{-1}) = 3409; 2925; 1703; 1601; 1514; 1407; 1174; 1108; 1068; 827; 768; 527. M.p > 170ºC (decompose).

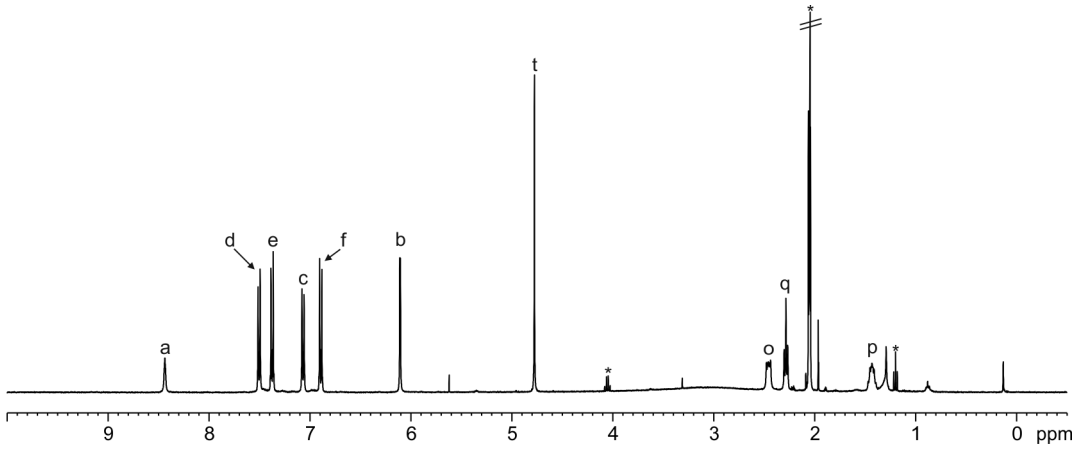

Figure S26. ^{1}H NMR (400 MHz, $(CD_3)_2CO$, 298 K) spectrum of **5**. See Figure S25 for proton assignment. *Solvent residual peaks.

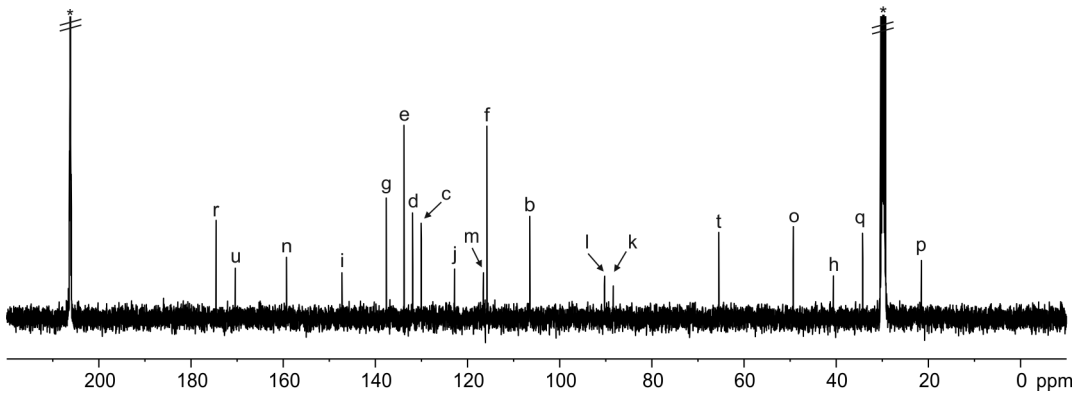

Figure S27. $^{13}C\{^{1}H\}$ NMR (100 MHz, $(CD_3)_2CO$, 298 K) spectrum of **5**. See Figure S25 for proton assignment. *Solvent residual peaks.

2.10 Octa-pyridinium octa-chloride super aryl-extended calix[4]pyrrole 6

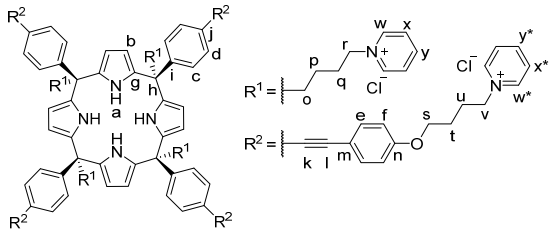

Figure S28. Line-drawing structure of **6**.

Octa-chloro super aryl-extended calix[4]pyrrole **4b** (30 mg, 0.02 mmol, 1 equiv.) was added to a dry-oven schlenk flask and kept under Argon atmosphere. Fresh distilled and dry pyridine (3 mL) was added and the reaction was stirred at 110ºC overnight. After that, the reaction was stopped and allowed to reach r.t. The crude was concentrated and CH_2Cl_2 (5 mL) was added and sonicated. The crude was filtered and washed with CH_2Cl_2 (3 mL) and hexane (3 mL) affording the product as a pale yellow solid (37 mg, 0.015 mmol, 90%). ^{1}H NMR (500 MHz with cryoprobe, CD_3OD, 298 K): δ (ppm) = 9.10-9.04 (m, 8H); 8.97-8.92 (m, 8H), 8.60-8.56 (m, 16H); 8.15-8.10 (m, 8H); 8.08-8.04 (m, 8H); 7.43-7.41 (m, 16H); 7.06-7.04 (m, 8H); 6.91-6.89 (m, 8H); 5.91 (s, 8H); 4.77-4.74 (m, 8H); 4.58-4.56 (m, 8H); 4.09 (t, J = 6.0 Hz, 8H); 2.50-2.48 (m, 8H); 2.27-2.22 (m, 8H); 2.00-1.97 (m, 8H); 1.91-1.88 (m, 8H); 1.26-1.22 (m, 8H). $^{13}C\{^{1}H\}$ NMR (125 MHz with cryoprobe, CD_3OD, 298 K): δ (ppm) = 160.4; 147.0; 146.8; 146.0; 145.9; 137.9; 134.1; 131.8; 129.9; 129.6; 129.5; 123.3; 116.7; 115.8; 106.8; 90.6; 88.6; 68.3; 62.8; 49.9; 40.2; 32.8; 29.5; 27.0; 23.2. HRMS (ESI-TOF) m/z: $[M\text{-}8Cl]^{8+}$ Calcd for $C_{148}H_{148}N_{12}O_4$ 269.6463; Found 269.6456. FTIR $\overline{\nu}$ (cm^{-1}) = 3209; 2936; 2865; 1632; 1601; 1513; 1485; 1283; 1246; 1174; 837; 774. M.p. > 235ºC (decompose).

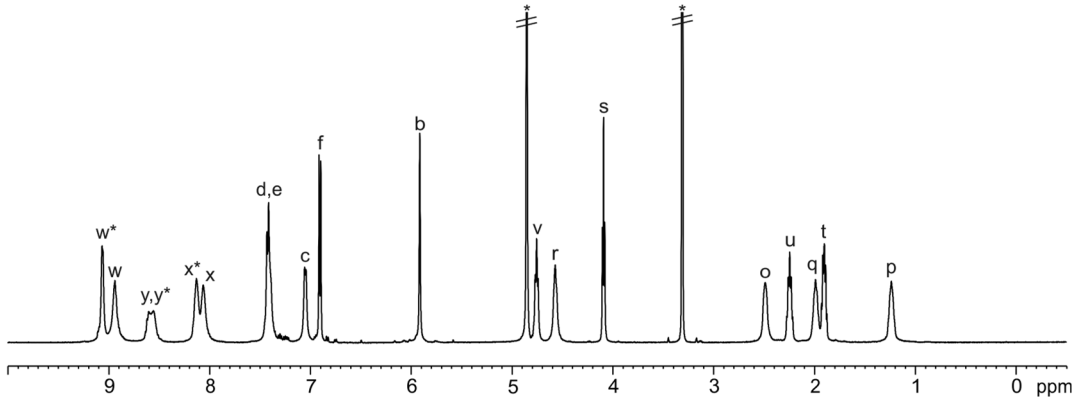

Figure S29. ^{1}H NMR (500 MHz with cryoprobe, CD_3OD, 298 K) spectrum of **6**. See Figure S28 for proton assignment. *Solvent residual peaks.

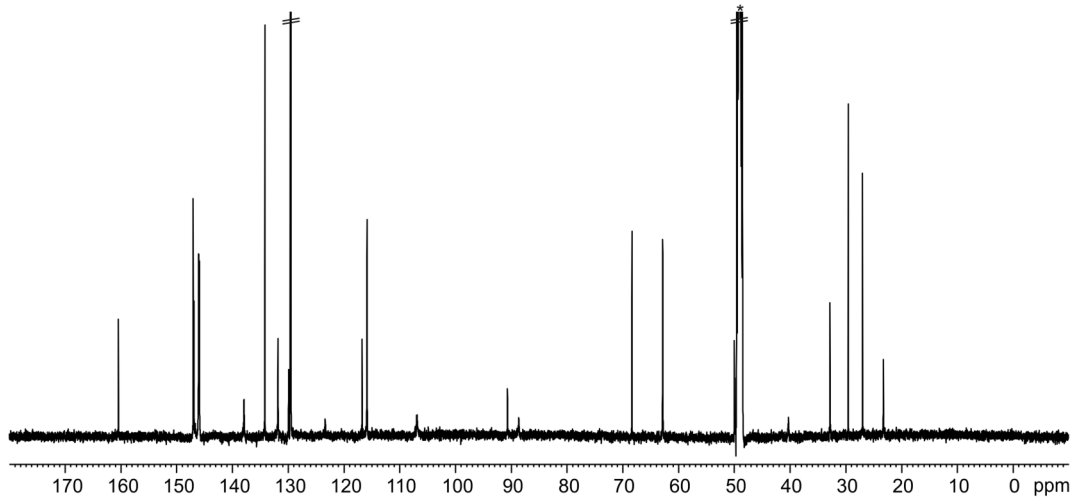

Figure S30. $^{13}C\{^{1}H\}$ NMR (125 MHz with cryoprobe, CD_3OD, 298 K) spectrum of **6**. *Solvent residual peak.

2.11 Octa-(1-methyl-1H-imidazolium) octa-chloride super aryl-extended calix[4]pyrrole 7

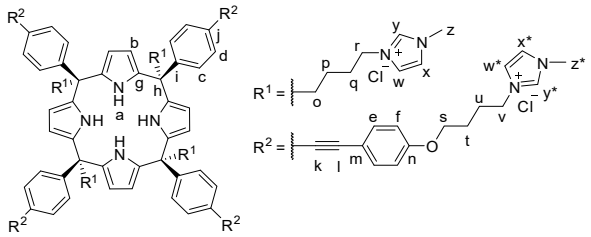

Figure S31. Line-drawing structure of **7**.

Octa-chloro super aryl-extended calix[4]pyrrole **4b** (35 mg, 0.02 mmol, 1 equiv.) was added to a dry-oven schlenk flask and kept under Argon atmosphere. 1-Methyl-1H-imidazole (3 mL) was added and the reaction was stirred at r.t. for 1 h. After that, the reaction was stirred at 110ºC overnight. Next, the reaction was stopped and allowed to reach r.t. The crude was concentrated to dryness and acetone (3 mL) was added and sonicated. The crude was filtered and the solid was washed with acetone (2x3 mL) and CH_2Cl_2 (2x3 mL) affording the product as a pale brown solid (40 mg, 0.016 mmol, 84%). ^{1}H NMR (500 MHz with cryoprobe, CD_3OD, 298 K): δ (ppm) = 9.00-8.90 (m, 8H); 7.69-7.67 (m, 4H); 7.57-7.42 (m, 24H); 7.10-7.00 (m, 8H); 6.90-6.89 (m, 8H); 5.91 (s, 8H); 4.33 (t, J = 7.2 Hz; 8H); 4.13-4.08 (m, 16H); 3.94-3.89 (m, 24H); 2.47 (s, 8H); 2.11 (t, J = 7.4 Hz, 8H); 1.87-1.84 (m, 16H); 1.19 (s, 8H). $^{13}C\{^{1}H\}$ NMR (125 MHz with cryoprobe, CD_3OD, 298 K): δ (ppm) = 160.5; 146.6; 137.9; 134.2; 131.8; 129.9; 125.0; 124.9; 123.6; 116.6; 115.8; 106.9; 90.6; 88.6; 68.3; 64.3; 54.8; 50.6; 40.3; 36.5; 31.4; 28.1; 27.1; 23.3. HRMS (ESI-TOF) m/z: $[M-8Cl]^{8+}$ Calcd for $C_{140}H_{156}N_{20}O_4$ 272.6572; Found 272.6564. FTIR $\overline{\nu}$ (cm^{-1}) = 3366; 3224; 3075; 2947; 1601; 1566; 1513; 1244; 1166; 1017; 833; 620. M.p. > 138ºC (decompose).

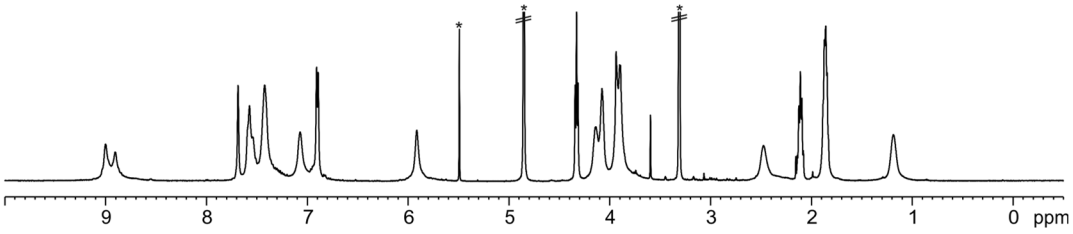

Figure S32. ^{1}H NMR (500 MHz with cryoprobe, CD_3OD, 298 K) spectrum of **7**. *Solvent residual peaks.

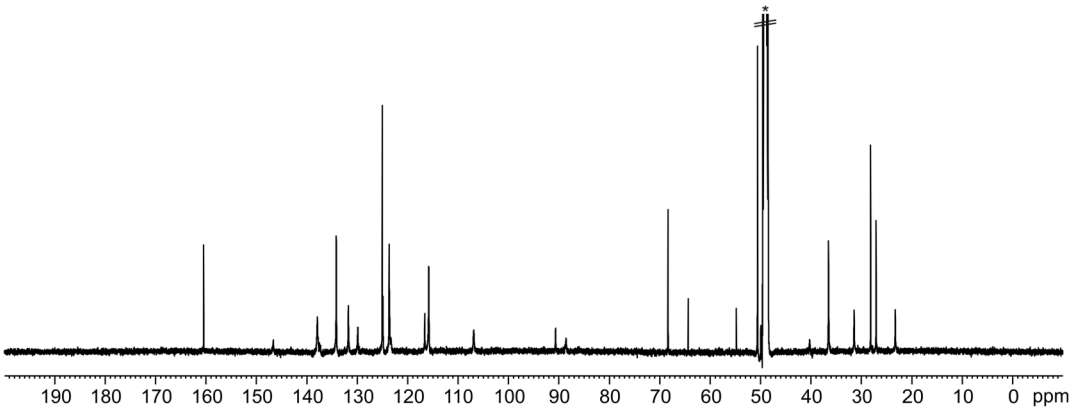

Figure S33. $^{13}C\{^{1}H\}$ NMR (125 MHz with cryoprobe, CD_3OD, 298 K) spectrum of **7**. *Solvent residual peak.

2.12 4-Butylpyridine *N*-oxide 8b

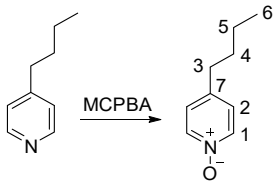

Scheme S2. Synthesis of 4-butylpyridine *N*-oxide **8b**.

4-Butylpyridine (0.22 g, 1.59 mmol, 1 equiv.) was dissolved in CH_2Cl_2 (21 mL). The solution was stirred at 0ºC and MCPBA (1.10 g, 4.77 mmol, 3 equiv.) was added portionwise. The reaction was stirred at 0ºC for 1 h and at r.t. for 2 h. The reaction was stopped and the crude was concentrated. The crude was purified by neutral alumina column chromatography (40 g, 95:5 CH_2Cl_2:IPA) affording the product as a pale brown oil (109 mg, 0.72 mmol, 45%). ^{1}H NMR (400 MHz, $CDCl_3$, 298 K): δ (ppm) = 8.11-8.09 (m, 2H); 7.07-7.05 (m, 2H), 2.58 (t, J = 7.6 Hz, 2H); 1.57 (tt, J = 7.6 Hz, J = 7.6 Hz, 2H); 1.33 (tq, J = 7.6 Hz, J = 7.6 Hz, 2H); 0.91 (t, J = 7.6 Hz, 3H). $^{13}C\{^{1}H\}$ NMR (100 MHz, $CDCl_3$, 298 K): δ (ppm) = 142.6; 138.8; 126.1; 34.2; 32.4; 22.2; 13.9. The synthesis and the analysis of **8b** by mass spectrometry were previously reported in the literature.[8]

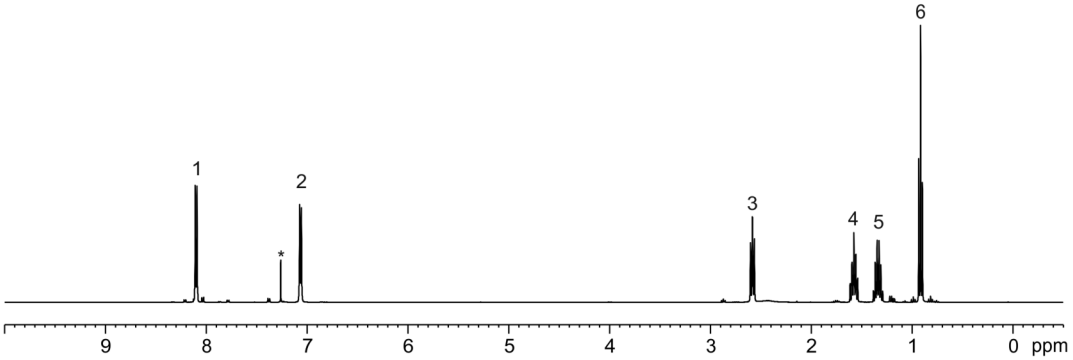

Figure S34. ^{1}H NMR (400 MHz, $CDCl_3$, 298 K) spectrum of **8b**. See Scheme S2 for proton assignment. *Solvent residual peak.

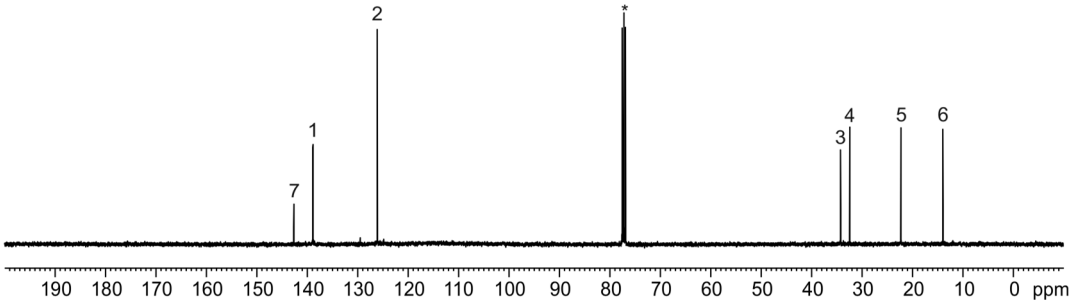

Figure S35. $^{13}C\{^{1}H\}$ NMR (100 MHz, $CDCl_3$, 298 K) spectrum of **8b**. See Scheme S2 for proton assignment. *Solvent residual peak.

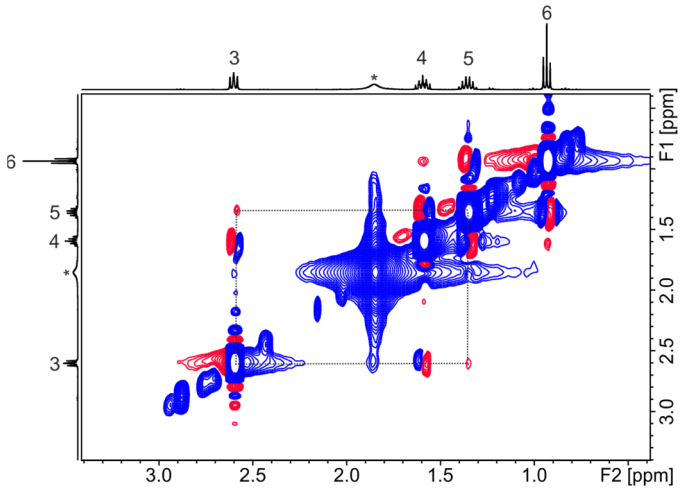

Figure S36. Selected region of the ^{1}H-^{1}H NOESY NMR (400 MHz, $CDCl_3$, 298 K, t_{mix} = 0.3 s) spectrum of **8b**. NOE cross-peaks were observed between H^3 and H^5. See Scheme S2 for proton assignment. *Solvent residual peak.

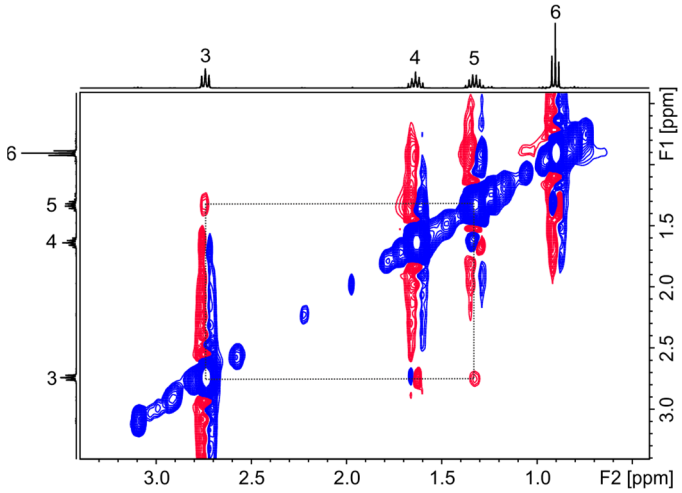

Figure S37. Selected region of the ^{1}H-^{1}H NOESY NMR (400 MHz, D_2O, 298 K, t_{mix} = 0.3 s) spectrum of **8b**. NOE cross-peaks were observed between H^3 and H^5. See Scheme S2 for proton assignment.

2.13 4-*tert*-Butylpyridine *N*-oxide 8c

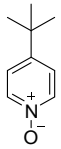

Figure S38. Line-drawing structure of **8c**.

4-*tert*-Butylpyridine *N*-oxide **8c** was prepared following a similar procedure previously described in literature.[9]

3. 2D DOSY and water-suppression NMR experiments of octa-acid 5

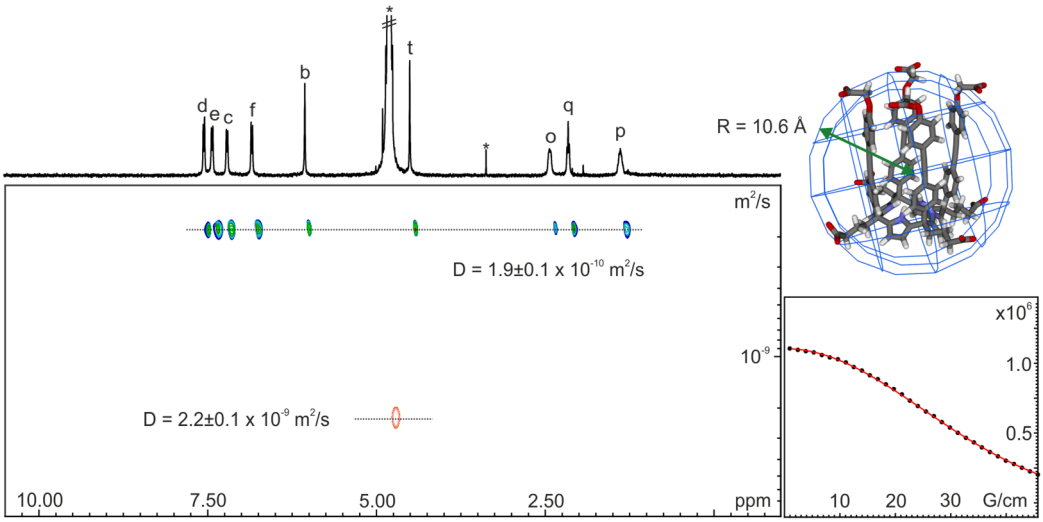

Figure S39. (left) Pseudo 2D plot of ^{1}H DOSY (500 MHz with cryoprobe, D_2O, pD ~ 10, 298 K, P30 = 1000 μs, D20 = 0.15 s) of **5** (1 mM); (right) Decay of proton b fitted to a mono-exponential function using Dynamics Center from Bruker. Hydrodynamic radius, R = 10.6 Å, was obtained from the diffusion constant using the Stokes-Einstein equation. The diffusion constant of water is in agreement with that reported in literature (2.3 x 10^{-9} m^2/s).[10] See Figure S25 for proton assignments. *Solvent residual peak.

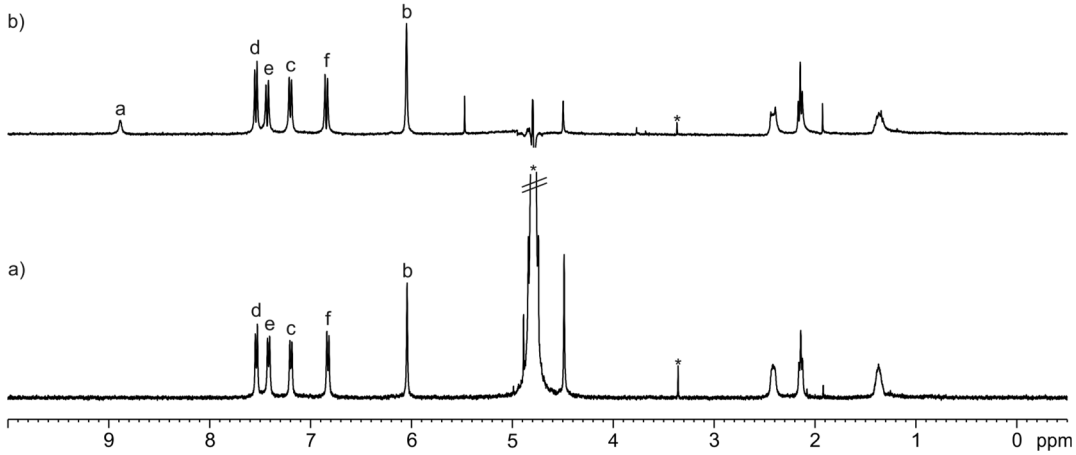

Figure S40. ^{1}H NMR (400 MHz, 298 K) of **5** (1 mM) in: a) D_2O and b) 9:1 H_2O:D_2O (water-suppression pulse sequence). See Figure S25 for proton assignment. *Solvent residual peaks.

4. Dilution and variable-temperature (VT) ^{1}H NMR experiments of 6 and 7

4.1 ^{1}H NMR spectra of octa-pyridinium 6 in $(CD_3)_2SO$

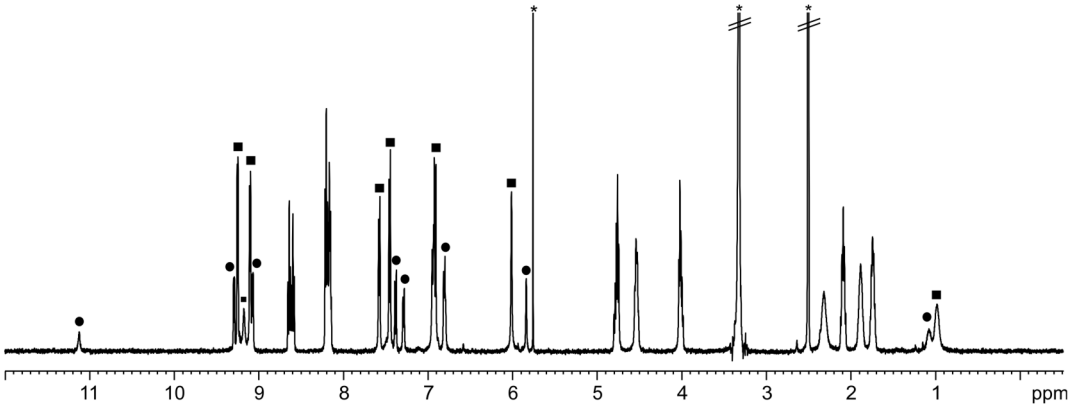

Figure S41. ^{1}H NMR (400 MHz, $(CD_3)_2SO$, 298 K) spectrum of **6**. The ^{1}H NMR spectrum showed two set of signals in a 70:30 molar ratio, which are assigned to the protons of free SAE-C[4]P (squares) and Cl^-⊂SAE-C[4]P (circles), respectively. *Solvent residual peaks.

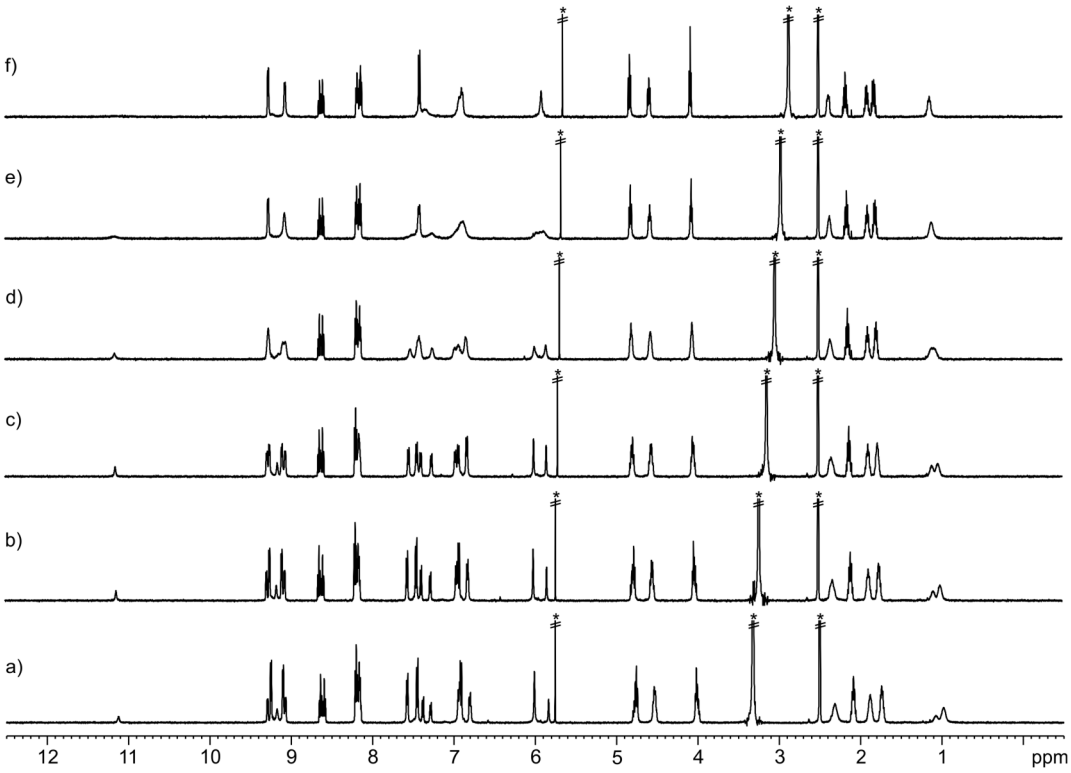

Figure S42. VT ^{1}H NMR (500 MHz, $(CD_3)_2SO$) spectra of **6** at: a) 298 K; b) 318 K; c) 338 K; d) 358 K; e) 373 K and f) 393 K. *Solvent residual peaks.

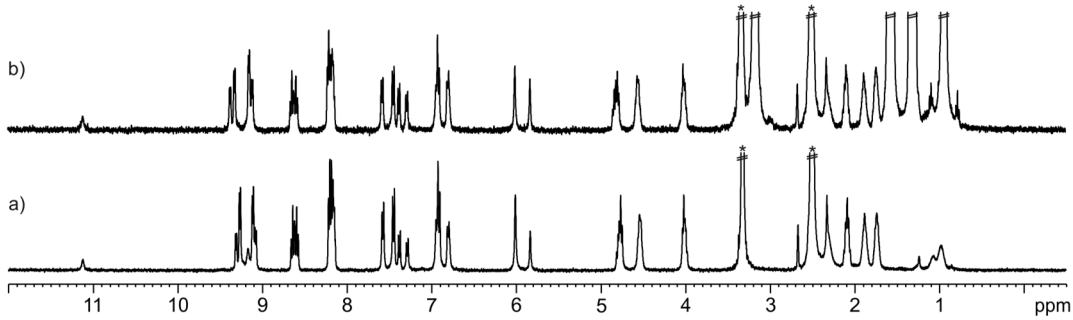

Figure S43. ^{1}H NMR (400 MHz, $(CD_3)_2SO$, 298 K) spectra of **6** and TBACl: a) **6** and b) TBACl + **6** (20:1 molar ratio). The spectrum b) showed two set of signals in a 60:40 molar ratio, which are assigned to the protons of free SAE-C[4]P and Cl^-⊂SAE-C[4]P, respectively. *Solvent residual peaks.

4.2 ^{1}H NMR spectra of octa-(1-methyl-1H-imidazolium) 7 in $(CD_3)_2SO$

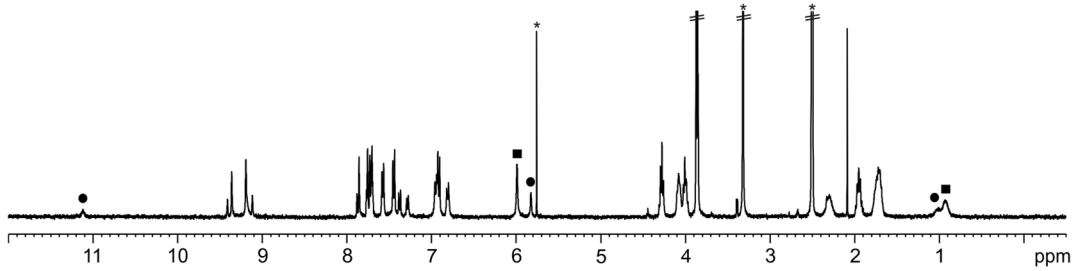

Figure S44. ^{1}H NMR (400 MHz, $(CD_3)_2SO$, 298 K) spectrum of **7**. The ^{1}H NMR spectrum showed two set of signals in a 70:30 molar ratio, which are assigned to the protons of free SAE-C[4]P (squares) and Cl^-⊂SAE-C[4]P (circles), respectively. *Solvent residual peaks.

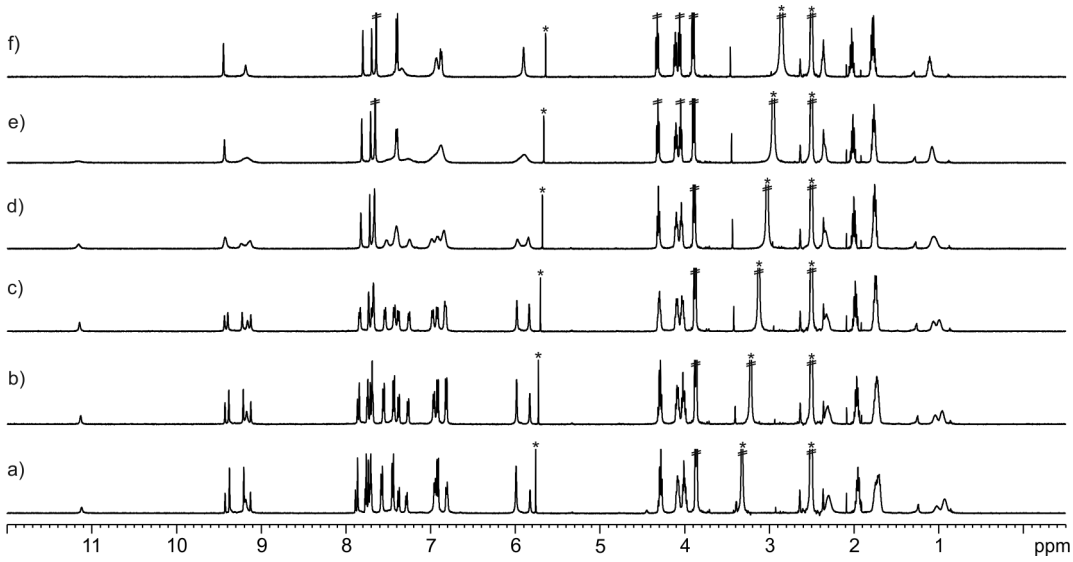

Figure S45. VT ^{1}H NMR (500 MHz, $(CD_3)_2SO$) spectra of **7** at: a) 298 K; b) 318 K; c) 338 K; d) 358 K; e) 373 K and f) 393 K. *Solvent residual peaks.

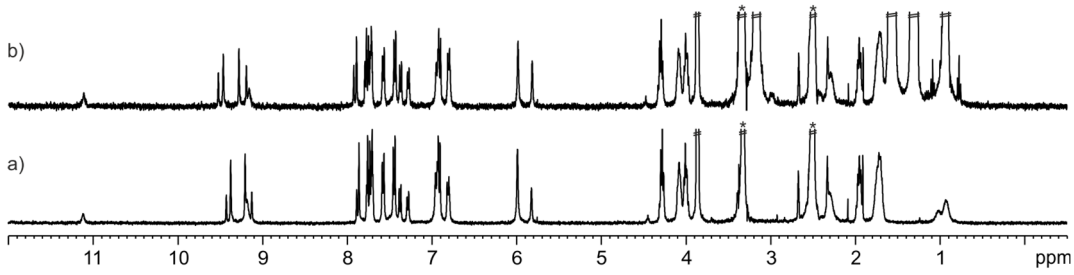

Figure S46. ^{1}H NMR (400 MHz, $(CD_3)_2SO$, 298 K) spectra of **7** and TBACl: a) **7** and b) TBACl + **7** (20:1 molar ratio). The spectrum b) showed two set of signals in a 60:40 molar ratio, which are assigned to the protons of free SAE-C[4]P and Cl^-⊂SAE-C[4]P, respectively. *Solvent residual peaks.

4.3 Dilution experiment of octa-pyridinium 6 in water

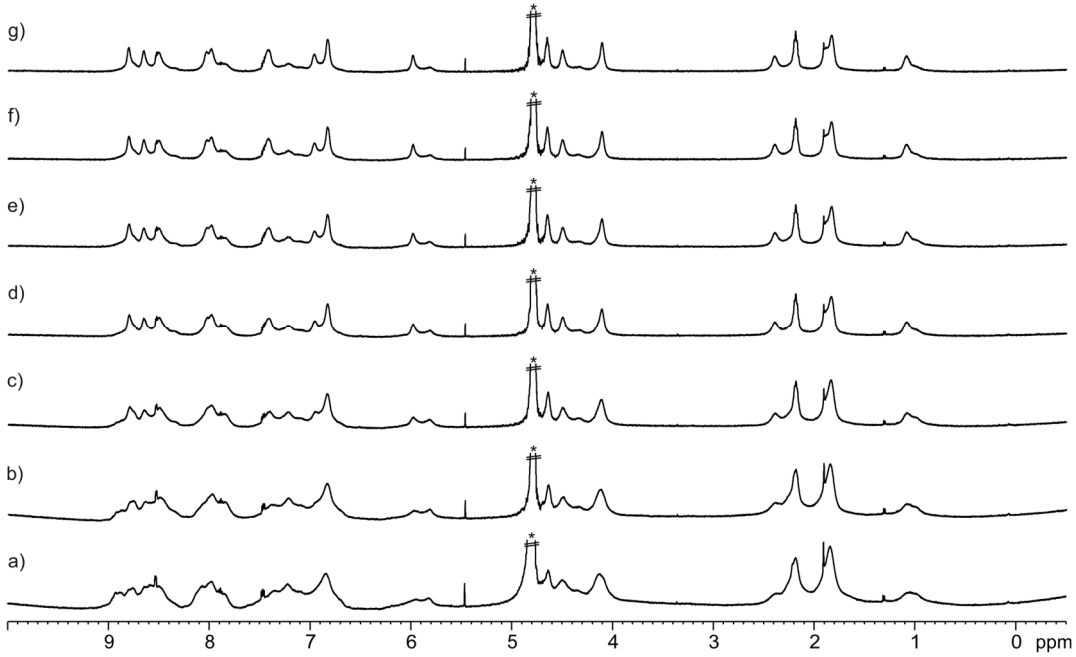

Figure S47. ^{1}H NMR (500 MHz with cryoprobe, D_2O, 298 K) spectra of **6**: a) 1 mM; b) 0.8 mM; c) 0.6 mM; d) 0.4 mM; e) 0.2 mM; f) 0.1 mM and g) 0.05 mM. *Solvent residual peak.

4.4 Dilution experiment of octa-(1-methyl-1H-imidazolium) 7 in water

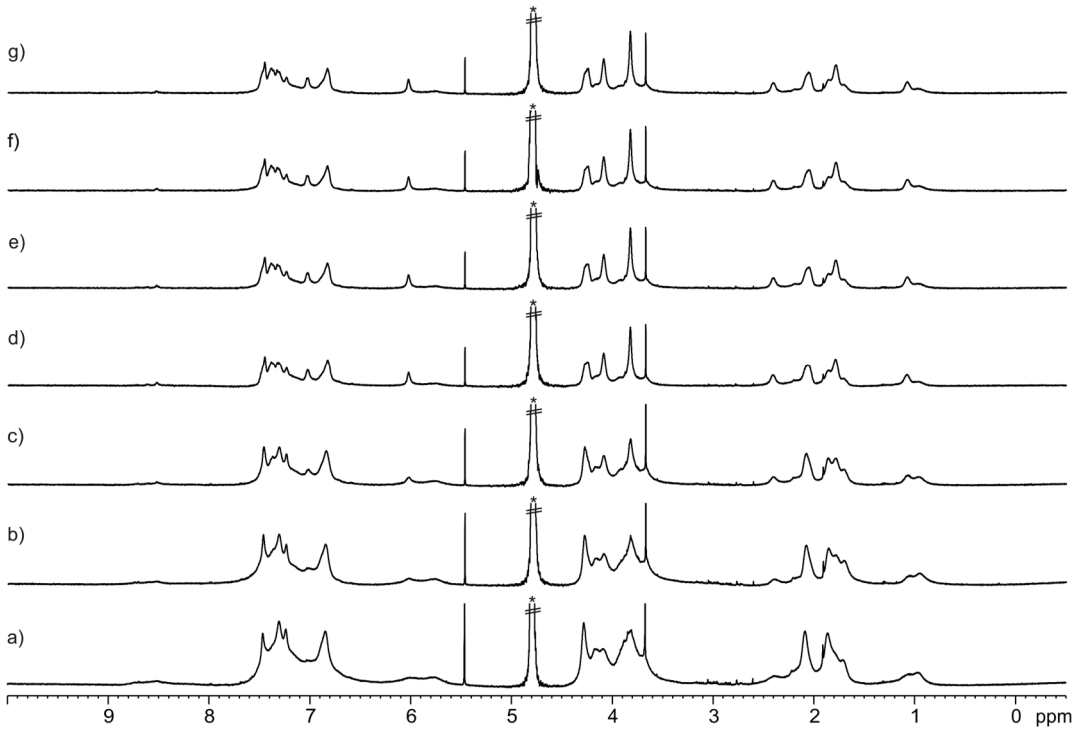

Figure S48. ^{1}H NMR (500 MHz with cryoprobe, D_2O, 298 K) spectra of **7**: a) 1 mM; b) 0.8 mM; c) 0.6 mM; d) 0.4 mM; e) 0.2 mM; f) 0.1 mM and g) 0.05 mM. *Solvent residual peak.

4.5 VT ^{1}H NMR experiment of octa-pyridinium 6 in water

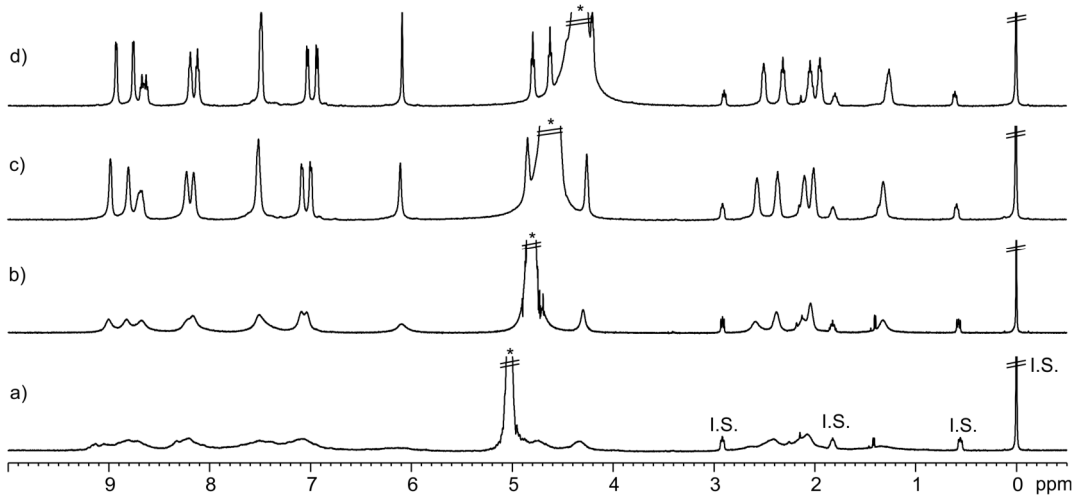

Figure S49. VT ^{1}H NMR (500 MHz, D_2O) spectra of **6** at: a) 298 K; b) 318 K; c) 338 K and d) 358 K. Sodium 3-(trimethylsilyl)propane-1-sulfonate (I.S.). *Solvent residual peak.

4.6 VT ^{1}H NMR experiment of octa-(1-methyl-1H-imidazolium) 7 in water

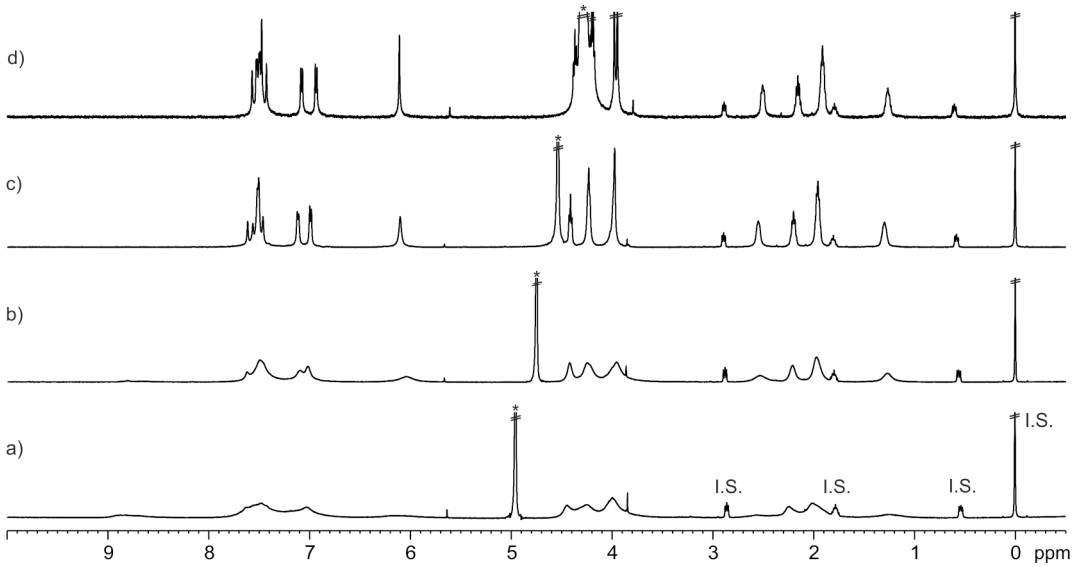

Figure S50. VT ^{1}H NMR (500 MHz, D_2O) spectra of **7** at: a) 298 K; b) 318 K; c) 338 K and d) 358 K. Sodium 3-(trimethylsilyl)propane-1-sulfonate (I.S.). *Solvent residual peak.

5. ^{1}H NMR spectroscopic titration experiments of octa-acid 5 with pyridyl *N*-oxides

A solution of host **5** (1 mM) was prepared in D_2O at pD ~ 10 using NaOD. Subsequently, 0.5 mL of the solution were transferred to a NMR tube. The remaining D_2O solution of the host was used to prepare the titrant's solution, which contained the pyridyl *N*-oxide **8a-f** at 20-30 fold higher concentration ([G] = 20-30 mM and [**5**] = 1 mM). In this manner, the concentration of the host was maintained constant throughout the titration. Immediately, the 0.5 mL of the host solution was titrated by manually injecting incremental amounts of the titrant's solution using a micro syringe. A ^{1}H NMR spectrum of the mixture was acquired after each injection and vigorous hand shaking of the NMR tube for few seconds.

4-Phenylpyridine *N*-oxide 8a

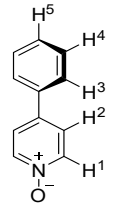

Figure S51. Line-drawing structure of **8a**.

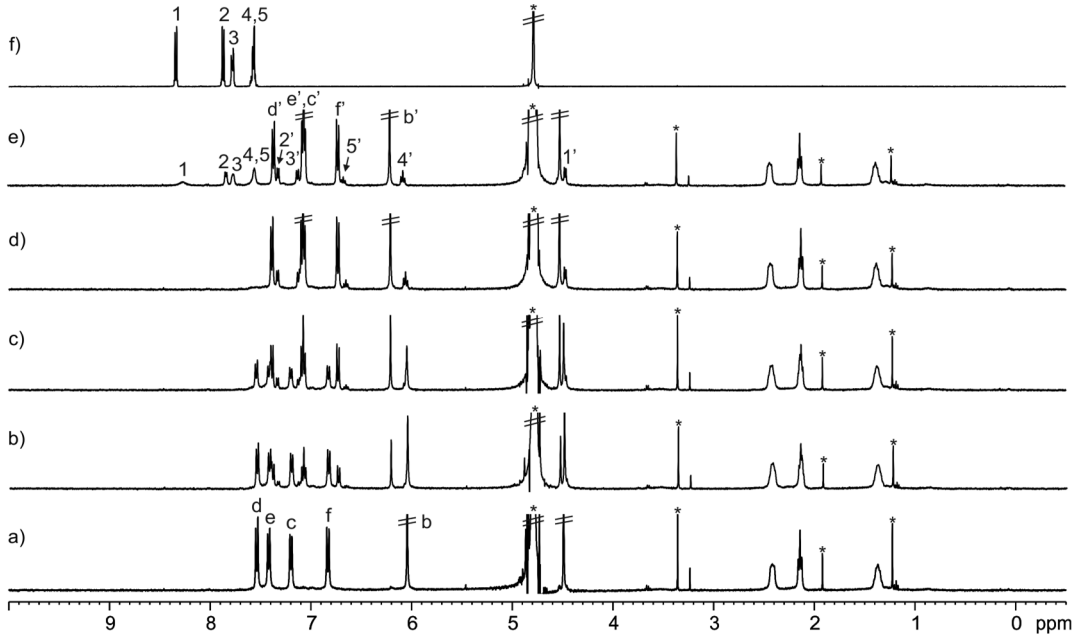

Figure S52. ^{1}H NMR (400 MHz, D_2O, pD ~ 10, 298 K) spectra of **5** and **8a**: a) **5**; b) **8a** + **5** (0.4:1 molar ratio); c) **8a** + **5** (0.65:1 molar ratio); d) **8a** + **5** (1:1 molar ratio); e) **8a** + **5** (1.8:1 molar ratio) and f) **8a**. See Figure S25 and Figure S51 for proton assignments. Primed letters and numbers correspond to proton signals of bound components. *Solvent residual peaks.

Table S3. Chemical shifts of the proton signals of **8a** (δ, ppm) and complexation-induced chemical shifts ($\Delta\delta$, ppm).

Signal	δ_{free}	δ_{bound}	$\Delta\delta$
1	8.27	4.42	-3.85
2	7.83	7.27	-0.56
3	7.75	7.08	-0.67
4	7.53	6.05	-1.48
5	7.53	6.64	-0.89

4-Butylpyridine *N*-oxide 8b

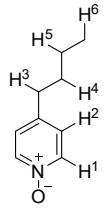

Figure S53. Line-drawing structure of **8b**.

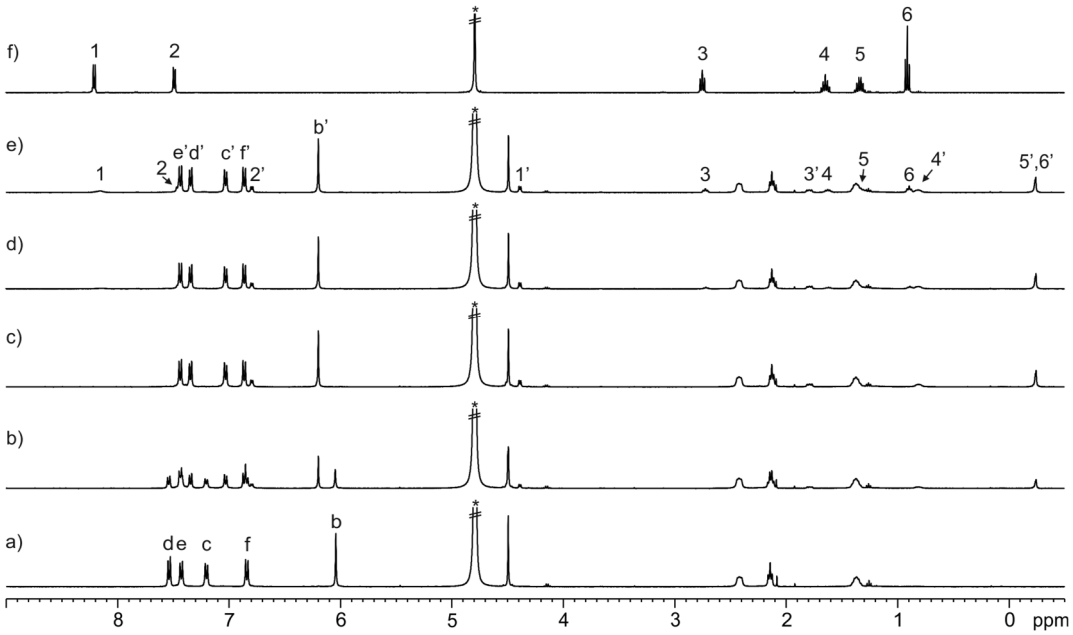

Figure S54. ^{1}H NMR (400 MHz, D_2O, pD ~ 10, 298 K) spectra of **5** and **8b**: a) **5**; b) **8b** + **5** (0.55:1 molar ratio); c) **8b** + **5** (1:1 molar ratio); d) **8b** + **5** (1.4:1 molar ratio); e) **8b** + **5** (2:1 molar ratio) and f) **8b**. See Figure S25 and Figure S53 for proton assignments. Primed letters and numbers correspond to proton signals of bound components. *Solvent residual peak.

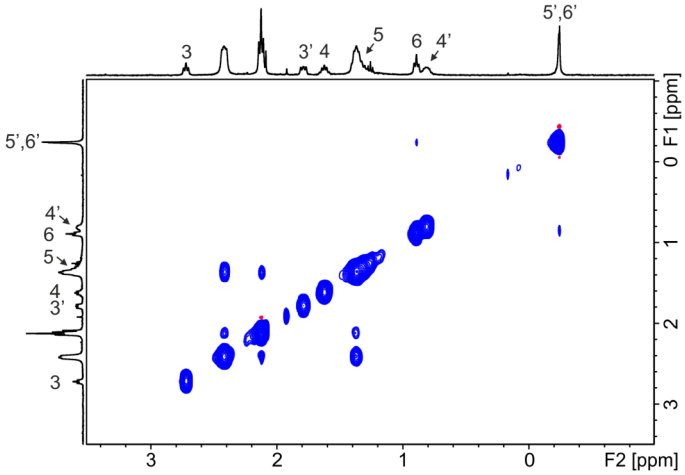

Figure S55. ^{1}H-^{1}H NOESY NMR (400 MHz, D_2O, pD ~ 10, 298 K, t_{mix} = 0.6 s) spectrum of **8b** and **5** (2:1 molar ratio). Primed numbers correspond to proton signals of bound component. See Figure S53 for proton assignments.

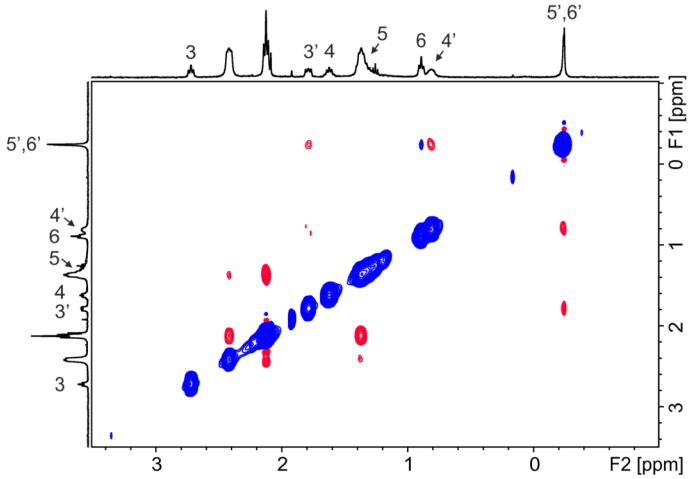

Figure S56. ^{1}H-^{1}H ROESY NMR (400 MHz, D_2O, pD ~ 10, 298 K, spin-lock = 0.4 s) spectrum of **8b** and **5** (2:1 molar ratio). Primed numbers correspond to proton signals of bound component. See Figure S53 for proton assignments.

Table S4. Chemical shifts of the proton signals of **8b** (δ, ppm) and complexation-induced chemical shifts ($\Delta\delta$, ppm).

Signal	δ_{free}	δ_{bound}	$\Delta\delta$
1	8.21	4.38	-3.83
2	7.49	6.79	-0.70
3	2.75	1.79	-0.96
4	1.65	0.81	-0.84
5	1.33	-0.24	-1.57
6	0.91	-0.24	-1.15

4-*tert*-Butylpyridine *N*-oxide 8c

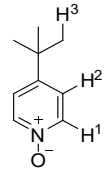

Figure S57. Line-drawing structure of **8c**.

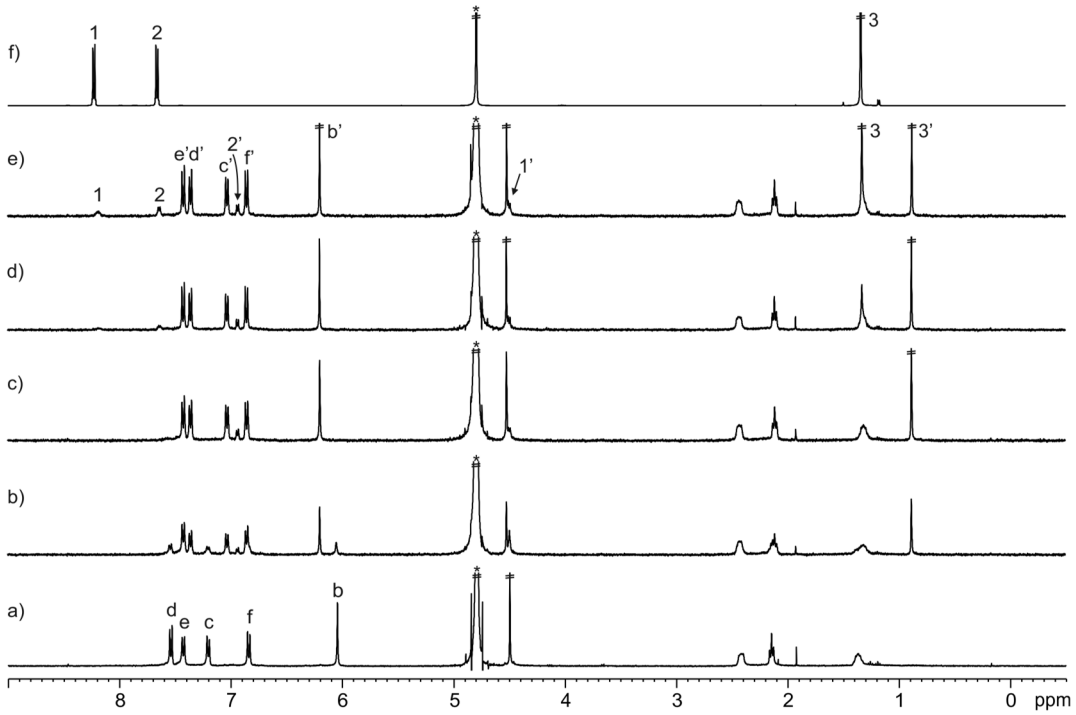

Figure S58. ^{1}H NMR (400 MHz, D_2O, pD ~ 10, 298 K) spectra of **5** and **8c**: a) **5**; b) **8c** + **5** (0.7:1 molar ratio); c) **8c** + **5** (1:1 molar ratio); d) **8c** + **5** (1.6:1 molar ratio); e) **8c** + **5** (2.2:1 molar ratio) and f) **8c**. Primed letters and numbers correspond to proton signals of bound components. See Figure S25 and Figure S57 for proton assignments. *Solvent residual peak.

Table S5. Chemical shifts of the proton signals of **8c** (δ, ppm) and complexation-induced chemical shifts ($\Delta\delta$, ppm).

Signal	δ_{free}	δ_{bound}	$\Delta\delta$
1	8.23	4.50	-3.73
2	7.66	6.94	-0.72
3	1.34	0.88	-0.46

4-Methylpyridine *N*-oxide 8d

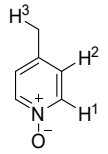

Figure S59. Line-drawing structure of **8d**.

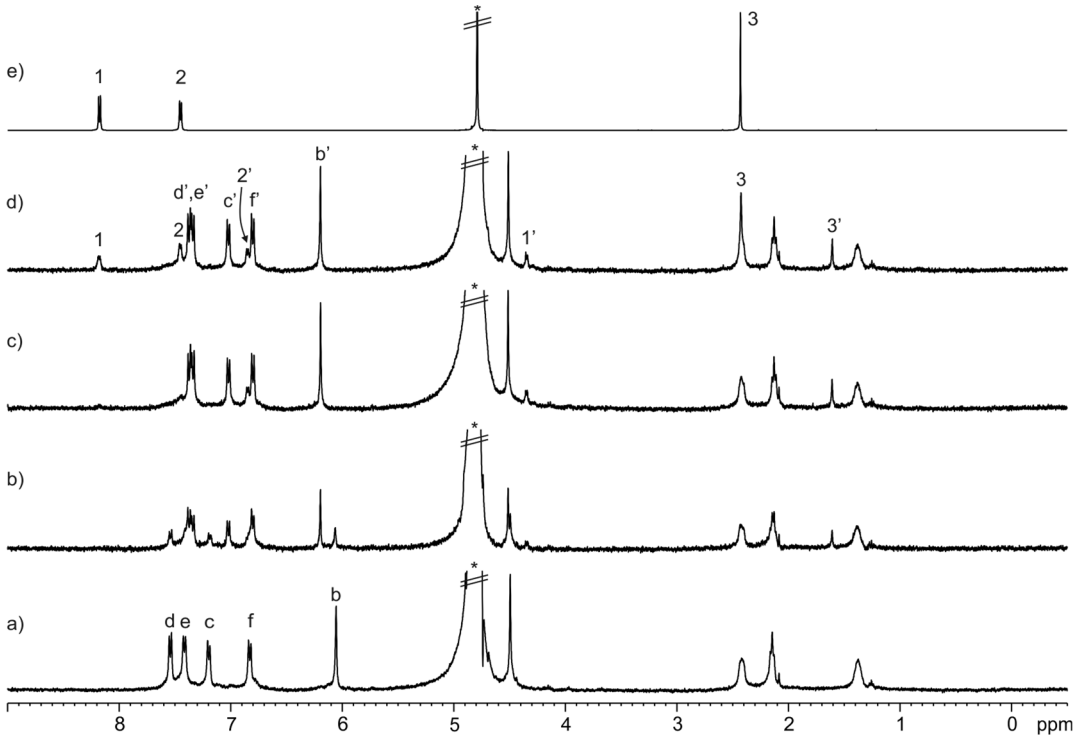

Figure S60. ^{1}H NMR (400 MHz, D_2O, pD ~ 10, 298 K) spectra of **5** and **8d**: a) **5**; b) **8d** + **5** (0.6:1 molar ratio); c) **8d** + **5** (1:1 molar ratio); d) **8d** + **5** (2.2:1 molar ratio) and e) **8d**. Primed letters and numbers correspond to proton signals of bound components. See Figure S25 and Figure S59 for proton assignments.*Solvent residual peak.

Table S6. Chemical shifts of the proton signals of **8d** (δ, ppm) and complexation-induced chemical shifts ($\Delta\delta$, ppm).

Signal	δ_{free}	δ_{bound}	$\Delta\delta$
1	8.18	4.35	-3.83
2	7.45	6.85	-0.60
3	2.43	1.61	-0.82

Pyridine *N*-oxide 8e

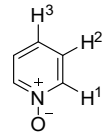

Figure S61. Line-drawing structure of **8e**.

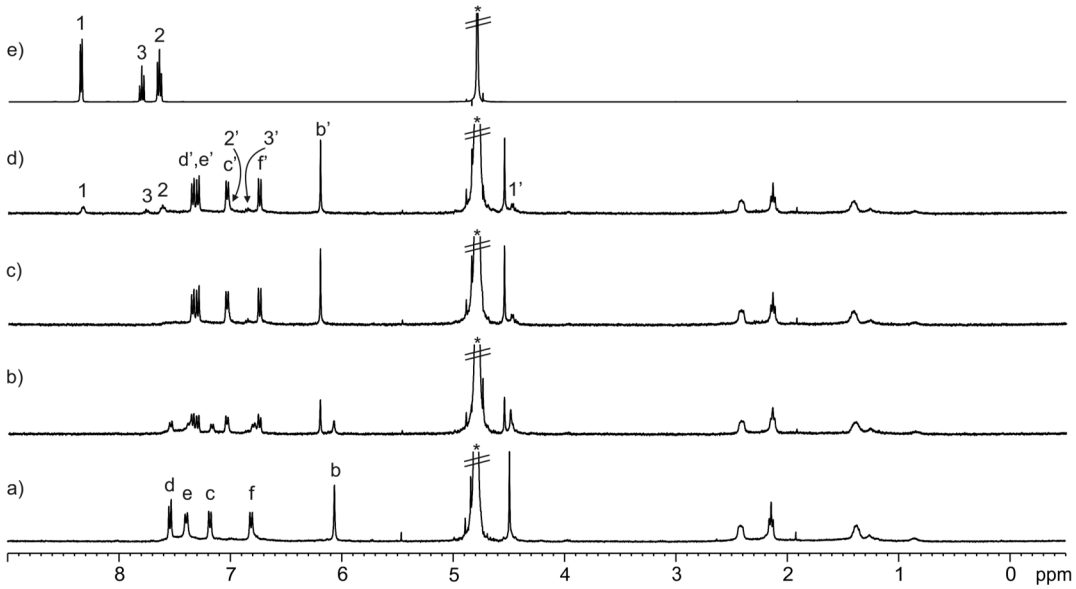

Figure S62. ^{1}H NMR (400 MHz, D_2O, pD ~ 10, 298 K) spectra of **5** and **8e**: a) **5**; b) **8e** + **5** (0.6:1 molar ratio); c) **8e** + **5** (1:1 molar ratio); d) **8e** + **5** (2.2:1 molar ratio) and e) **8e**. Primed letters and numbers correspond to proton signals of bound components. See Figure S25 and Figure S61 for proton assignments. *Solvent residual peak.

Table S7. Chemical shifts of the proton signals of **8e** (δ, ppm) and complexation-induced chemical shifts ($\Delta\delta$, ppm).

Signal	δ_{free}	δ_{bound}	$\Delta\delta$
1	8.33	4.47	-3.86
2	7.62	7.02	-0.60
3	7.76	6.85	-0.91

Isoquinoline *N*-oxide 8f

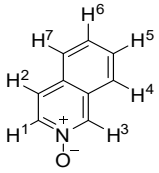

Figure S63. Line-drawing structure of **8f**.

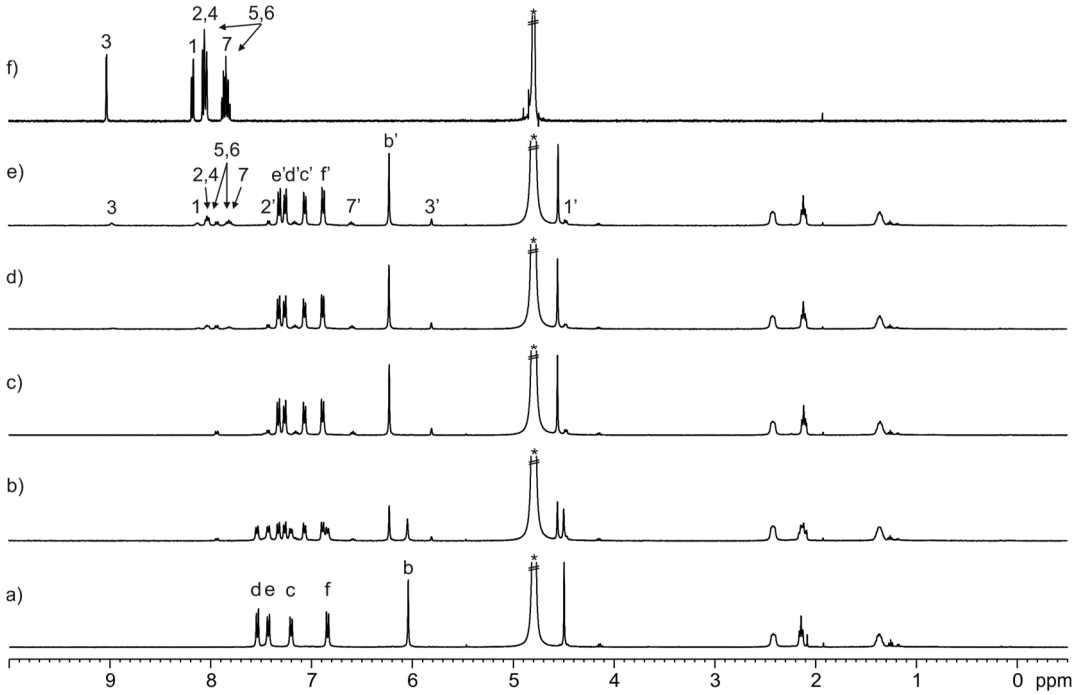

Figure S64. ^{1}H NMR (400 MHz, D_2O, pD ~ 10, 298 K) spectra of **5** and **8f**: a) **5**; b) **8f** + **5** (0.55:1 molar ratio); c) **8f** + **5** (1:1 molar ratio); d) **8f** + **5** (1.4:1 molar ratio); e) **8f** + **5** (1.9:1 molar ratio) and f) **8f**. Primed letters and numbers correspond to proton signals of bound components. See Figure S25 and Figure S63 for proton assignments. *Solvent residual peak.

Table S8. Chemical shifts of the proton signals of **8f** (δ, ppm) and complexation-induced chemical shifts ($\Delta\delta$, ppm).

Signal	δ_{free}	δ_{bound}	$\Delta\delta$
1	8.13	4.47	-3.66
2	8.03	7.42	-0.61
3	8.98	5.80	-3.18
7	7.82	6.60	-1.22

6. Pair-wise ^{1}H NMR competitive experiments of octa-acid 5 with pyridyl *N*-oxides

A series of pair-wise NMR competitive titration experiments were performed using receptor **5** (1 mM) and the pyridyl *N*-oxides **8a-f** in basic (pD ~ 10) D_2O solutions. The binding constant ratio between the two competing complexes was determined by integration of selected proton signals in the acquired ^{1}H NMR spectra (K_{a2}/K_{a1} = ([HG_2]x[G_1])/([HG_1]x[G_2]). The binding constant values of the thermodynamically more stable complexes (K_a > 10^7 M^{-1}) were determined using the calculated ratio of the binding constants and the binding constant value of one of the complexes, which was measured either accurately by ITC experiments or from a previous pair-wise competitive experiment.

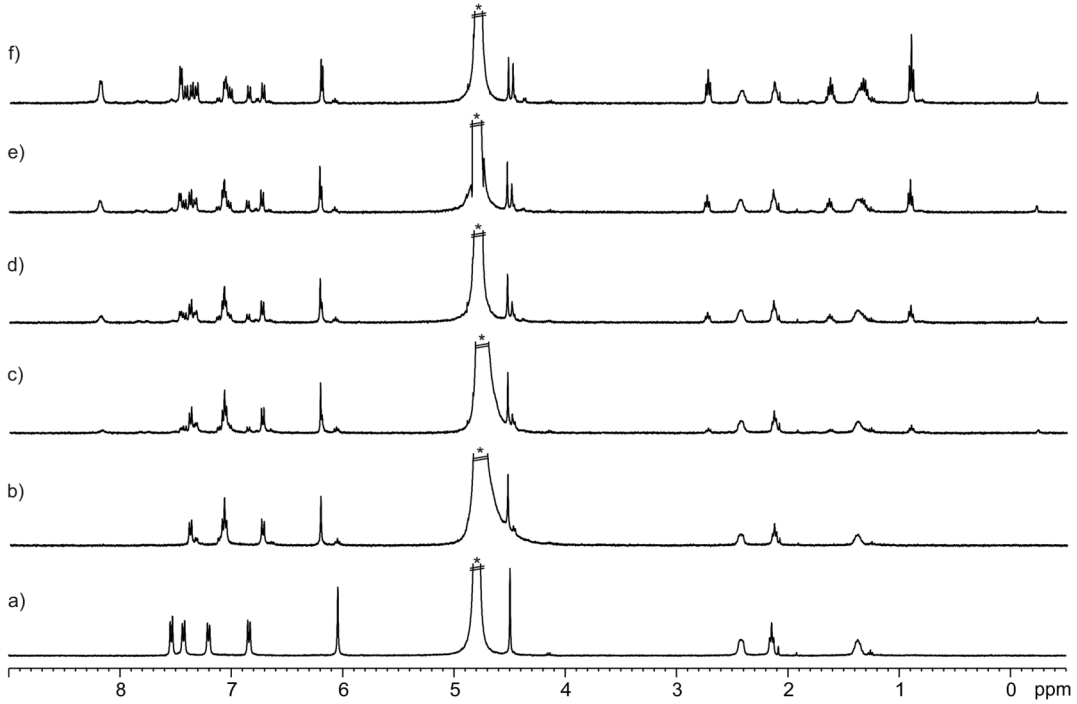

Figure S65. ^{1}H NMR (400 MHz, D_2O, pD ~ 10, 298 K) spectra of the pair-wise competitive experiment of **5**, **8a** and **8b**: a) **5**; b) **8a** + **5** (1:1 molar ratio); c) **8b** + **8a** + **5** (1:1:1 molar ratio); d) **8b** + **8a** + **5** (2:1:1 molar ratio); e) **8b** + **8a** + **5** (3:1:1 molar ratio) and f) **8b** + **8a** + **5** (5:1:1 molar ratio). *Solvent residual peak.

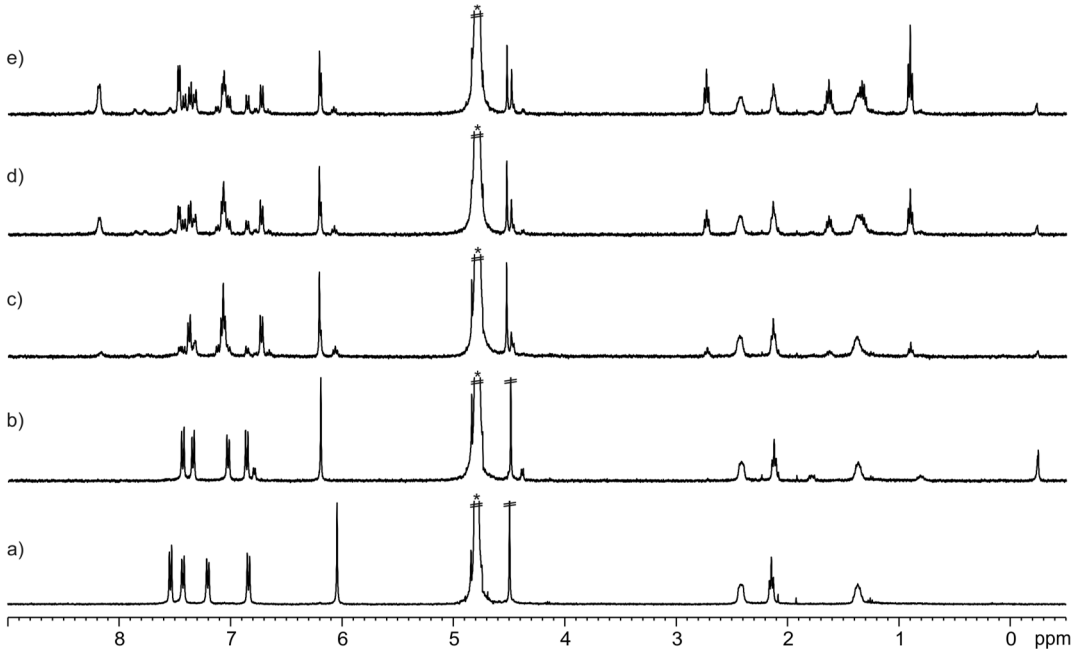

Figure S66. ^{1}H NMR (400 MHz, D_2O, pD ~ 10, 298 K) spectra of the pair-wise competitive experiment of **5**, **8a** and **8b**: a) **5**; b) **8b** + **5** (1:1 molar ratio); c) **8a** + **8b** + **5** (1.1:1:1 molar ratio); d) **8a** + **8b** + **5** (1.1:2.8:1 molar ratio) and e) **8a** + **8b** + **5** (1.1:4.7:1 molar ratio). *Solvent residual peak.

Integration of selected proton signals in the spectra of the pair-wise competitive experiments indicated that K_a (**8a**⊂**5**) = 12±1 x K_a (**8b**⊂**5**).

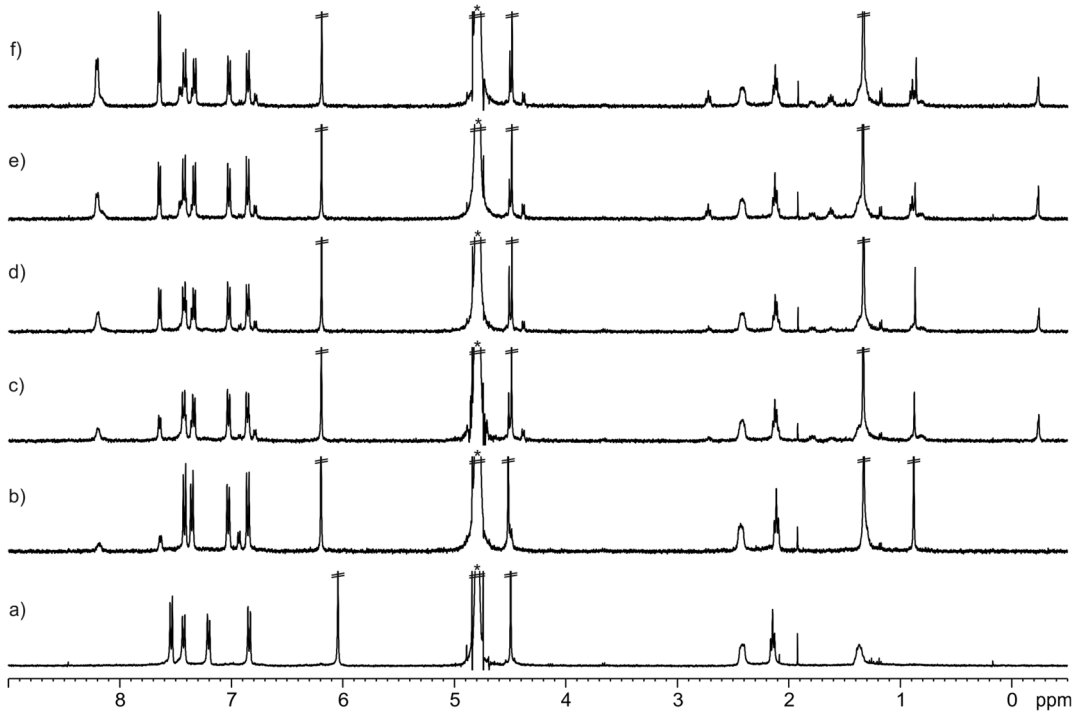

Figure S67. ^{1}H NMR (400 MHz, D_2O, pD ~ 10, 298 K) spectra of the pair-wise competitive experiment of **5**, **8b** and **8c**: a) **5**; b) **8c** + **5** (2.2:1 molar ratio); c) **8b** + **8c** + **5** (1.1:2.2:1 molar ratio); d) **8b** + **8c** + **5** (1.1:3.2:1 molar ratio); e) **8b** + **8c** + **5** (2.1:3.2:1 molar ratio) and f) **8b** + **8c** + **5** (2.1:5.3:1 molar ratio). *Solvent residual peak.

Integration of selected proton signals in the spectra of the pair-wise competitive experiments indicated that K_a (**8b**⊂**5**) = 11.0±0.5 x K_a (**8c**⊂**5**).

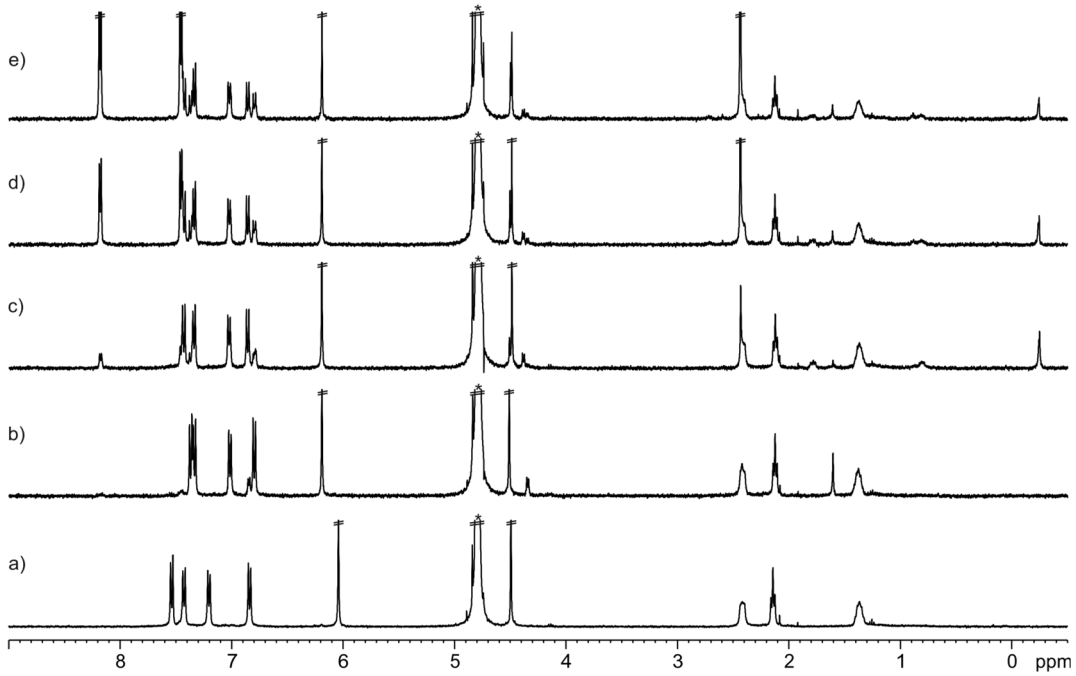

Figure S68. ^{1}H NMR (400 MHz, D_2O, pD ~ 10, 298 K) spectra of the pair-wise competitive experiment of **5**, **8b** and **8d**: a) **5**; b) **8d** + **5** (1.1:1 molar ratio); c) **8b** + **8d** + **5** (1:1.1:1 molar ratio); d) **8b** + **8d** + **5** (1:5.1:1 molar ratio) and e) **8b** + **8d** + **5** (1:11.4:1 molar ratio). *Solvent residual peak.

Integration of selected proton signals in the spectra of the pair-wise competitive experiments indicated that K_a (**8b**⊂**5**) = 50±20 x K_a (**8d**⊂**5**).

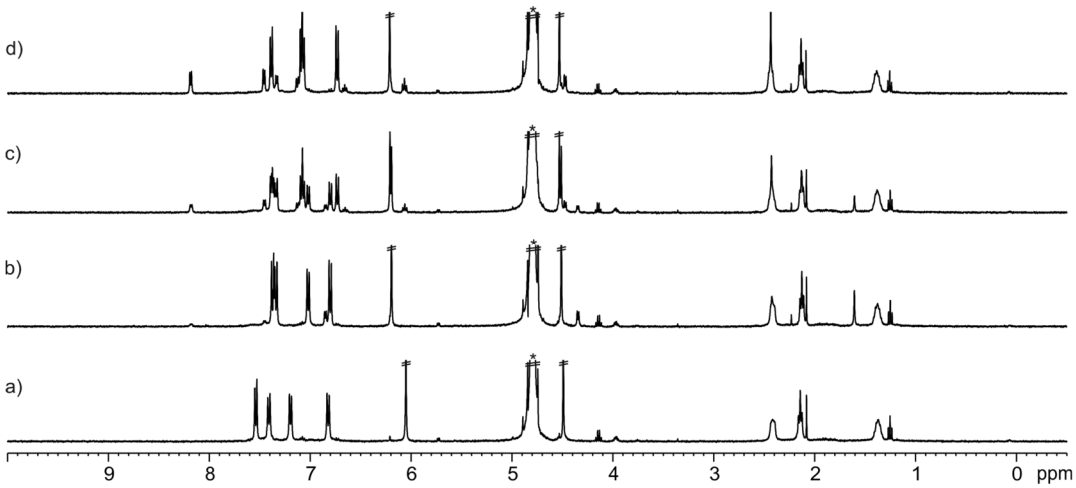

Figure S69. ^{1}H NMR (400 MHz, D_2O, pD ~ 10, 298 K) spectra of the pair-wise competitive experiment of **5**, **8a** and **8d**: a) **5**; b) **8d** + **5** (1.5:1 molar ratio); c) **8a** + **8d** + **5** (0.5:1.5:1 molar ratio) and d) **8a** + **8d** + **5** (1:1.5:1 molar ratio). *Solvent residual peak.

The spectra of the pair-wise competitive experiments indicated that K_a (**8a**⊂**5**) >> K_a (**8d**⊂**5**).

7. ^{1}H NMR spectroscopic titration experiments of octa-pyridinium 6 with pyridyl *N*-oxides

A solution of host **6** (1 mM) was prepared in D_2O. Subsequently, 0.5 mL of the solution were transferred to a NMR tube. The remaining D_2O solution of the host was used to prepare the titrant's solution, which contained the pyridyl *N*-oxide **8a-f** at 20-30 fold higher concentration ([G] = 20-30 mM and [**6**] = 1 mM). In this manner, the concentration of the host was maintained constant throughout the titration. Immediately, the 0.5 mL of the host solution was titrated by manually injecting incremental amounts of the titrant's solution using a micro syringe. A ^{1}H NMR spectrum of the mixture was acquired after each injection and vigorous hand shaking of the NMR tube for few seconds.

4-Phenylpyridine *N*-oxide 8a

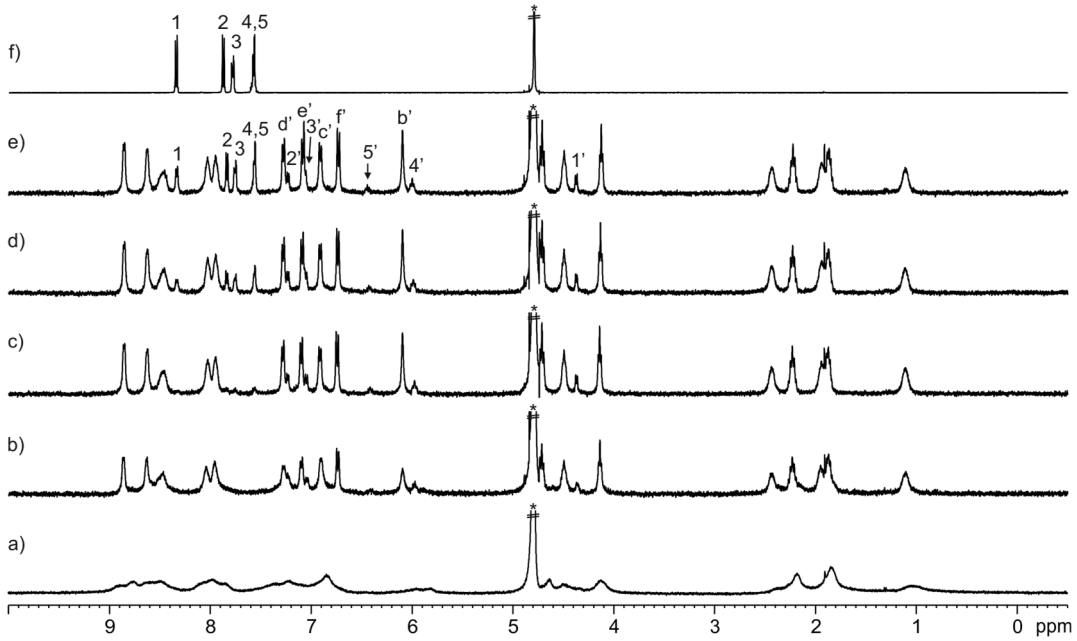

Figure S70. ^{1}H NMR (400 MHz, D_2O, 298 K) spectra of **6** and **8a**: a) **6**; b) **8a** + **6** (0.5:1 molar ratio); c) **8a** + **6** (1:1 molar ratio); d) **8a** + **6** (1.5:1 molar ratio); e) **8a** + **6** (2:1 molar ratio) and f) **8a**. Primed letters and numbers correspond to proton signals of bound components. See Figure S28 and Figure S51 for proton assignments. *Solvent residual peak.

Table S9. Chemical shifts of the proton signals of **8a** (δ, ppm) and complexation-induced chemical shifts ($\Delta\delta$, ppm).

Signal	δ_{free}	δ_{bound}	$\Delta\delta$
1	8.27	4.37	-3.90
2	7.83	7.23	-0.60
3	7.75	7.06	-0.69
4	7.53	6.00	-1.53
5	7.53	6.45	-1.08

4-Butylpyridine *N*-oxide 8b

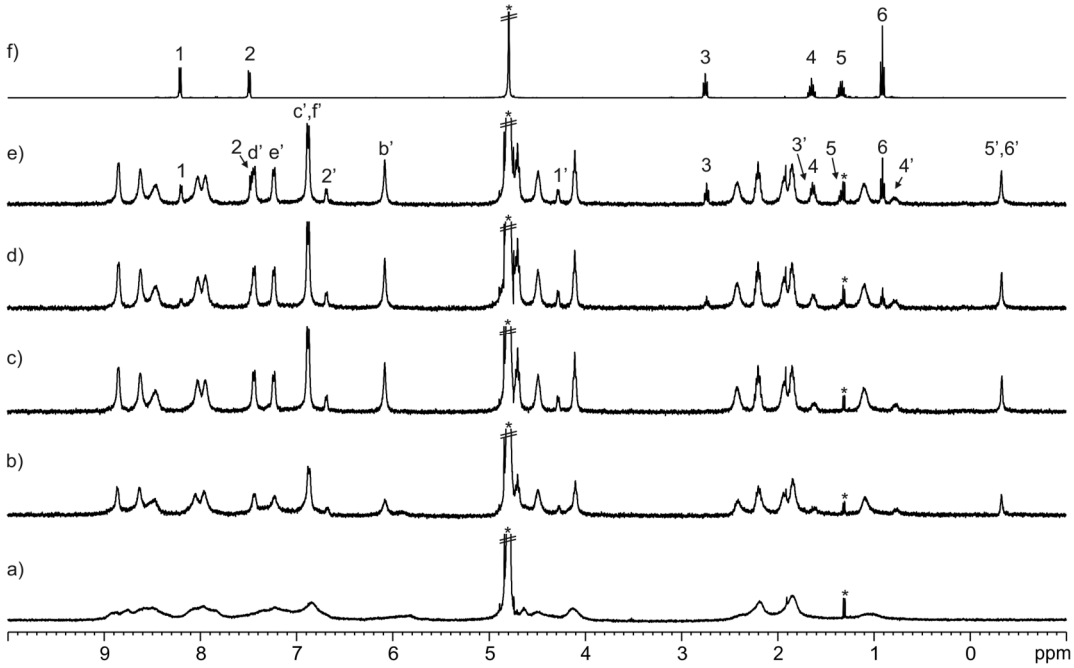

Figure S71. ^{1}H NMR (400 MHz, D_2O, 298 K) spectra of **6** and **8b**: a) **6**; b) **8b** + **6** (0.5:1 molar ratio); c) **8b** + **6** (1:1 molar ratio); d) **8b** + **6** (1.5:1 molar ratio); e) **8b** + **6** (2:1 molar ratio) and f) **8b**. Primed letters and numbers correspond to proton signals of bound components. See Figure S28 and Figure S53 for proton assignments. *Solvent residual peaks.

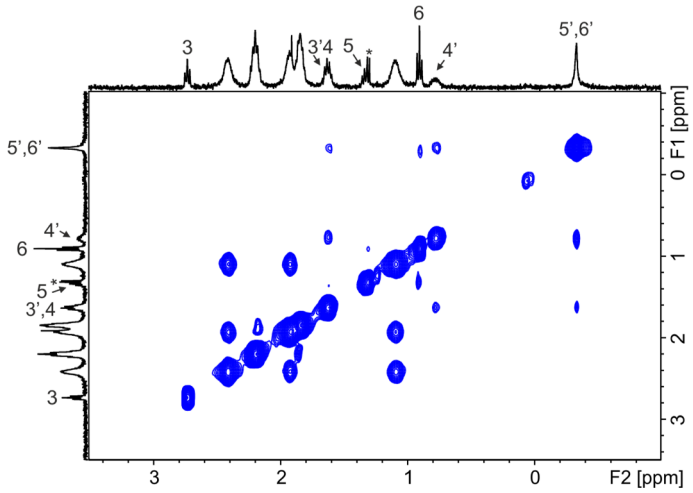

Figure S72. ^{1}H-^{1}H NOESY NMR (400 MHz, D_2O, 298 K, t_{mix} = 0.6 s) spectrum of **8b** and **6** (2:1 molar ratio). Primed numbers correspond to proton signals of bound component. See Figure S53 for proton assignments. *Solvent residual peak.

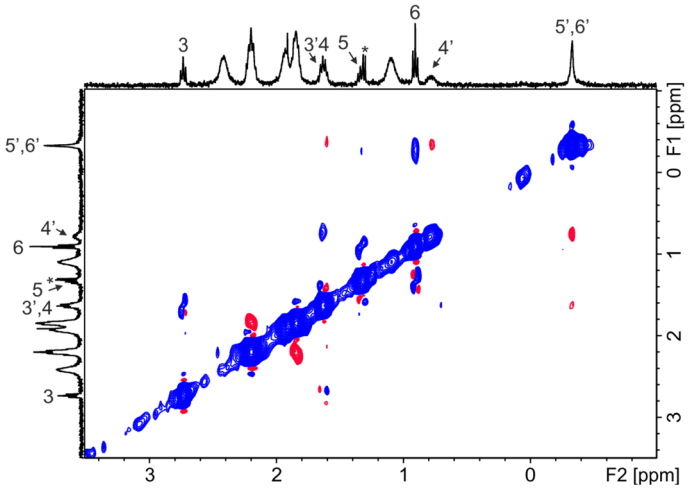

Figure S73. ^{1}H-^{1}H ROESY NMR (400 MHz, D_2O, 298 K, spin lock = 0.4 s) spectrum of **8b** and **6** (2:1 molar ratio). Primed numbers correspond to proton signals of bound component. See Figure S53 for proton assignments. *Solvent residual peak.

Table S10. Chemical shifts of the proton signals of **8b** (δ, ppm) and complexation-induced chemical shifts ($\Delta\delta$, ppm).

Signal	δ_{free}	δ_{bound}	$\Delta\delta$
1	8.21	4.28	-3.93
2	7.49	6.69	-0.80
3	2.75	1.64	-1.11
4	1.65	0.78	-0.87
5	1.33	-0.33	-1.66
6	0.91	-0.33	-1.24

4-*tert*-Butylpyridine *N*-oxide 8c

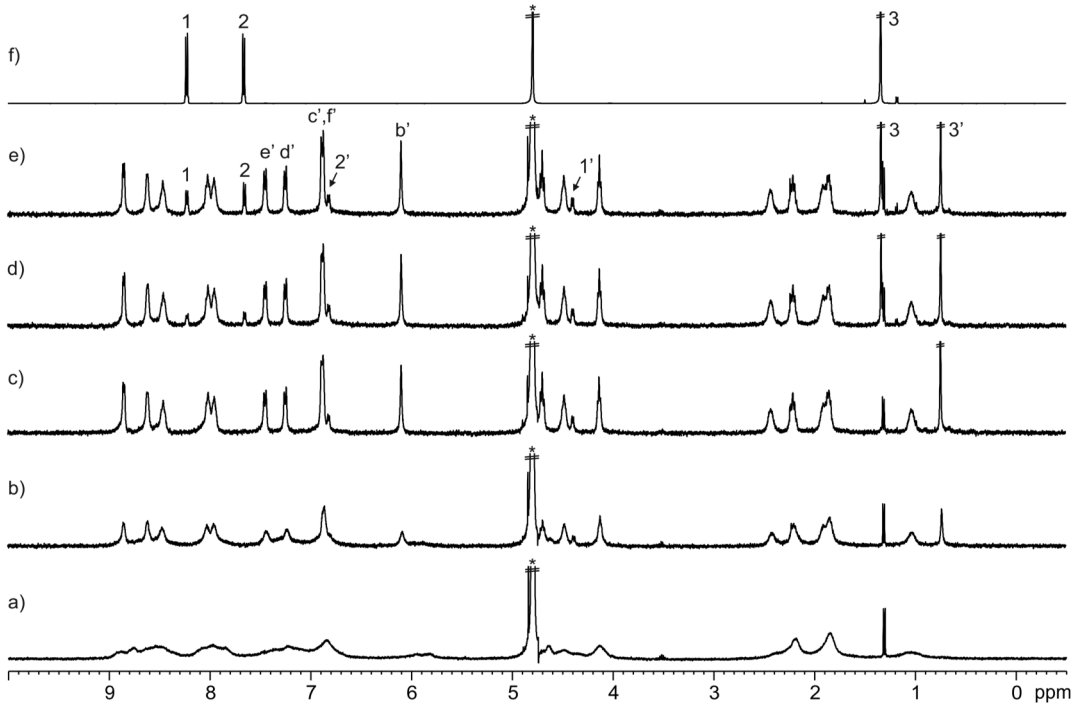

Figure S74. ^{1}H NMR (400 MHz, D_2O, 298 K) spectra of **6** and **8c**: a) **6**; b) **8c** + **6** (0.7:1 molar ratio); c) **8c** + **6** (1:1 molar ratio); d) **8c** + **6** (1.6:1 molar ratio); e) **8c** + **6** (2.2:1 molar ratio) and f) **8c**. Primed letters and numbers correspond to proton signals of bound components. See Figure S28 and Figure S57 for proton assignments. *Solvent residual peak.

Table S11. Chemical shifts of the proton signals of **8c** (δ, ppm) and complexation-induced chemical shifts ($\Delta\delta$, ppm).

Signal	δ_{free}	δ_{bound}	$\Delta\delta$
1	8.23	4.39	-3.84
2	7.66	6.82	-0.84
3	1.34	0.74	-0.60

4-Methylpyridine *N*-oxide 8d

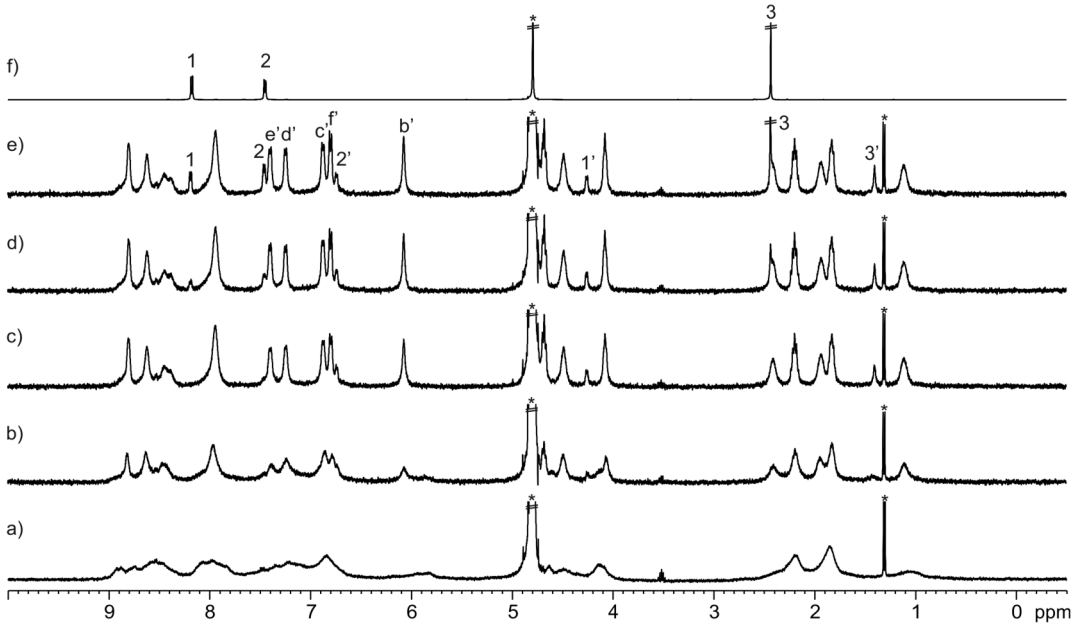

Figure S75. ^{1}H NMR (400 MHz, D_2O, 298 K) spectra of **6** and **8d**: a) **6**; b) **8d** + **6** (0.5:1 molar ratio); c) **8d** + **6** (1:1 molar ratio); d) **8d** + **6** (1.5:1 molar ratio); e) **8d** + **6** (2:1 molar ratio) and f) **8d**. Primed letters and numbers correspond to proton signals of bound components. See Figure S28 and Figure S59 for proton assignments. *Solvent residual peaks.

Table S12. Chemical shifts of the proton signals of **8d** (δ, ppm) and complexation-induced chemical shifts ($\Delta\delta$, ppm).

Signal	δ_{free}	δ_{bound}	$\Delta\delta$
1	8.18	4.26	-3.92
2	7.45	6.74	-0.71
3	2.43	1.40	-1.03

Pyridine *N*-oxide 8e

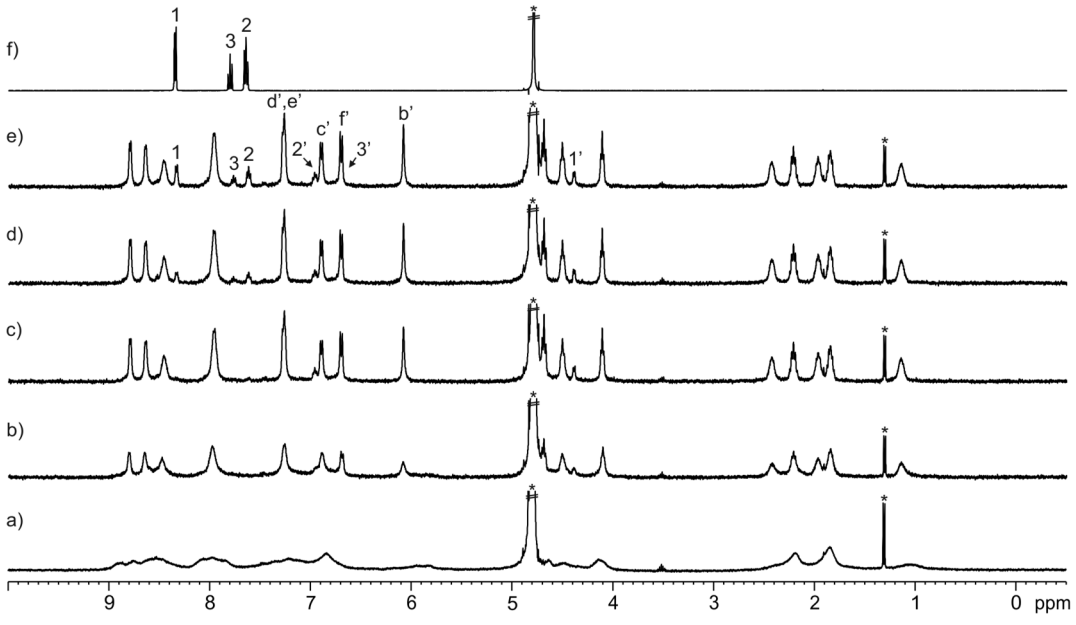

Figure S76. ^{1}H NMR (400 MHz, D_2O, 298 K) spectra of **6** and **8e**: a) **6**; b) **8e** + **6** (0.5:1 molar ratio); c) **8e** + **6** (1:1 molar ratio); d) **8e** + **6** (1.5:1 molar ratio); e) **8e** + **6** (2:1 molar ratio) and f) **8e**. Primed letters and numbers correspond to proton signals of bound components. See Figure S28 and Figure S61 for proton assignments. *Solvent residual peaks.

Table S13. Chemical shifts of the proton signals of **8e** (δ, ppm) and complexation-induced chemical shifts ($\Delta\delta$, ppm).

Signal	δ_{free}	δ_{bound}	$\Delta\delta$
1	8.35	4.39	-3.96
2	7.65	6.96	-0.69
3	7.80	6.70	-1.10

Isoquinoline *N*-oxide 8f

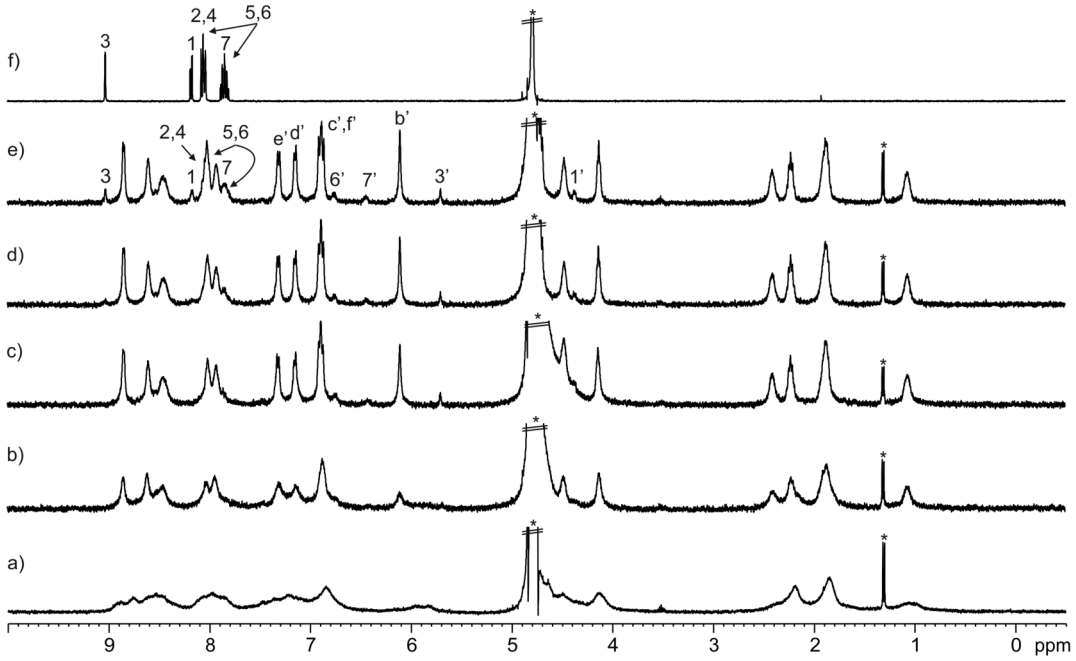

Figure S77. ^{1}H NMR (400 MHz, D_2O, 298 K) spectra of **6** and **8f**: a) **6**; b) **8f** + **6** (0.5:1 molar ratio); c) **8f** + **6** (1:1 molar ratio); d) **8f** + **6** (1.5:1 molar ratio); e) **8f** + **6** (2:1 molar ratio) and f) **8f**. Primed letters and numbers correspond to proton signals of bound components. See Figure S28 and Figure S63 for proton assignments. *Solvent residual peaks.

Table S14. Chemical shifts of the proton signals of **8f** (δ, ppm) and complexation-induced chemical shifts ($\Delta\delta$, ppm).

Signal	δ_{free}	δ_{bound}	$\Delta\delta$
1	8.16	4.37	-3.79
3	9.03	5.70	-3.33
6	7.84	6.76	-1.08
7	7.84	6.44	-1.40

8. Pair-wise ^{1}H NMR competitive experiments of octa-pyridinium 6 with pyridyl *N*-oxides

A series of pair-wise NMR competitive titration experiments were performed using receptor **6** (1 mM) and the pyridyl *N*-oxides **8a-f** in un-buffered D_2O solutions. The binding constant ratio between the two competing complexes was determined by integration of selected proton signals in the acquired ^{1}H NMR spectra (K_{a2}/K_{a1} = ([HG_2]x[G_1])/([HG_1]x[G_2]). The binding constant values of the thermodynamically more stable complexes (K_a > 10^7 M^{-1}) were determined using the calculated ratio of the binding constants and the binding constant value of one of the complexes, which was measured either accurately by ITC experiments or from a previous pair-wise competitive experiment.

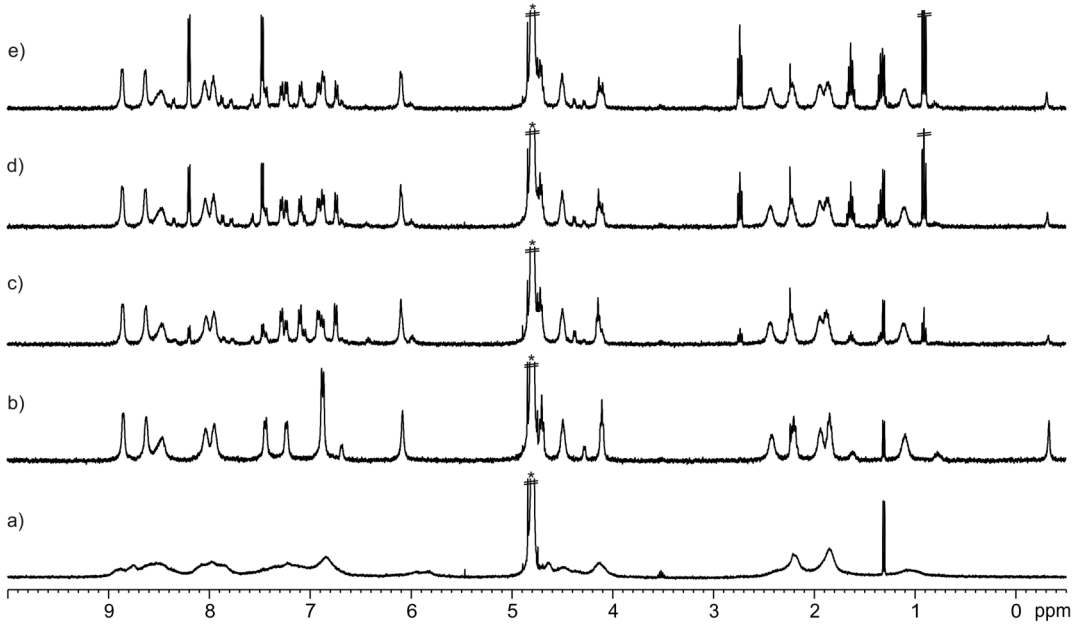

Figure S78. ^{1}H NMR (400 MHz, D_2O, 298 K) spectra of the pair-wise competitive experiment of **6**, **8a** and **8b**: a) **6**; b) **8b** + **6** (1:1 molar ratio); c) **8a** + **8b** + **6** (1.1:1:1 molar ratio); d) **8a** + **8b** + **6** (1.1:2.9:1 molar ratio) and e) **8a** + **8b** + **6** (1.1:4.4:1 molar ratio). *Solvent residual peak.

Integration of selected proton signals in the spectra of the pair-wise competitive experiments indicated that K_a (**8a**⊂**6**) = 7±1 x K_a (**8b**⊂**6**).

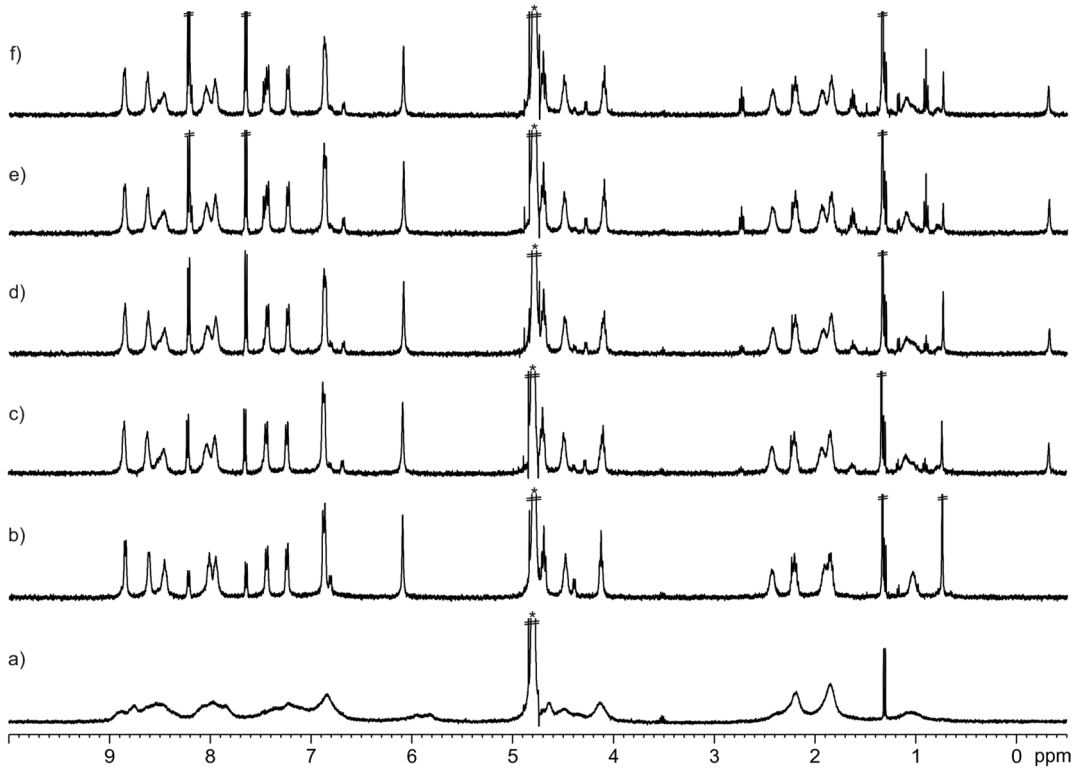

Figure S79. ^{1}H NMR (400 MHz, D_2O, 298 K) spectra of the pair-wise competitive experiment of **6**, **8b** and **8c**: a) **6**; b) **8c** + **6** (2.2:1 molar ratio); c) **8b** + **8c** + **6** (1:2.2:1 molar ratio); d) **8b** + **8c** + **6** (1:3.2:1 molar ratio); e) **8b** + **8c** + **6** (2:3.2:1 molar ratio) and f) **8b** + **8c** + **6** (2:5.6:1 molar ratio). *Solvent residual peak.

Integration of selected proton signals in the spectra of the pair-wise competitive experiments indicated that K_a (**8b**⊂**6**) = 10.0±0.5 x K_a (**8c**⊂**6**).

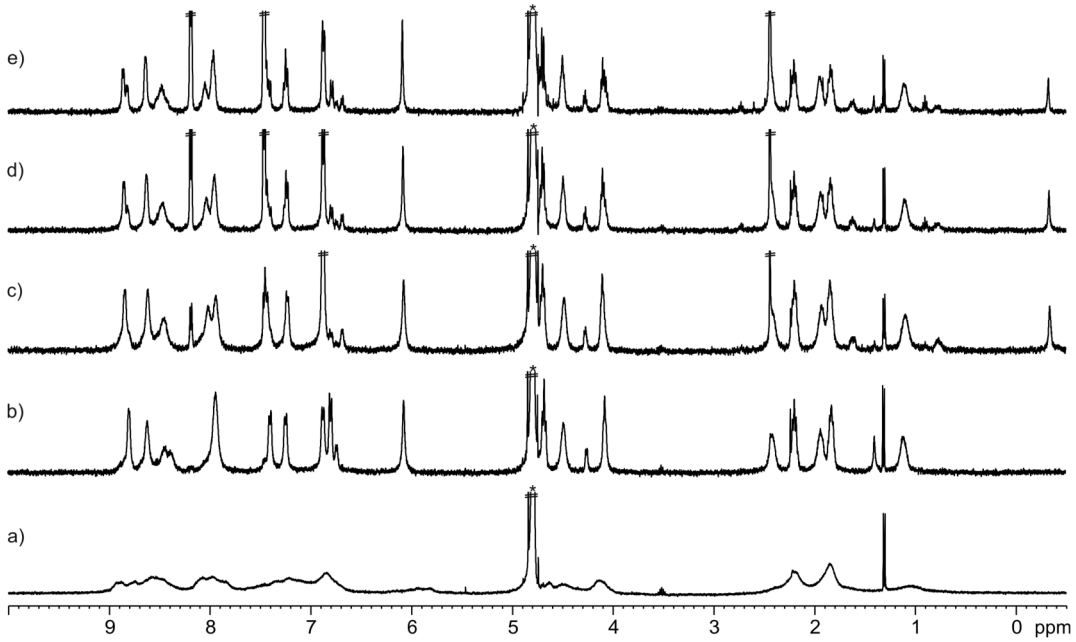

Figure S80. ^{1}H NMR (400 MHz, D_2O, 298 K) spectra of the pair-wise competitive experiment of **6**, **8b** and **8d**: a) **6**; b) **8d** + **6** (1.1:1 molar ratio); c) **8b** + **8d** + **6** (1:1.1:1 molar ratio); d) **8b** + **8d** + **6** (1:6:1 molar ratio) and e) **8b** + **8d** + **6** (1:12.7:1 molar ratio). *Solvent residual peak.

Integration of selected proton signals in the spectra of the pair-wise competitive experiments indicated that K_a (**8b**⊂**6**) = 60±10 x K_a (**8d**⊂**6**).

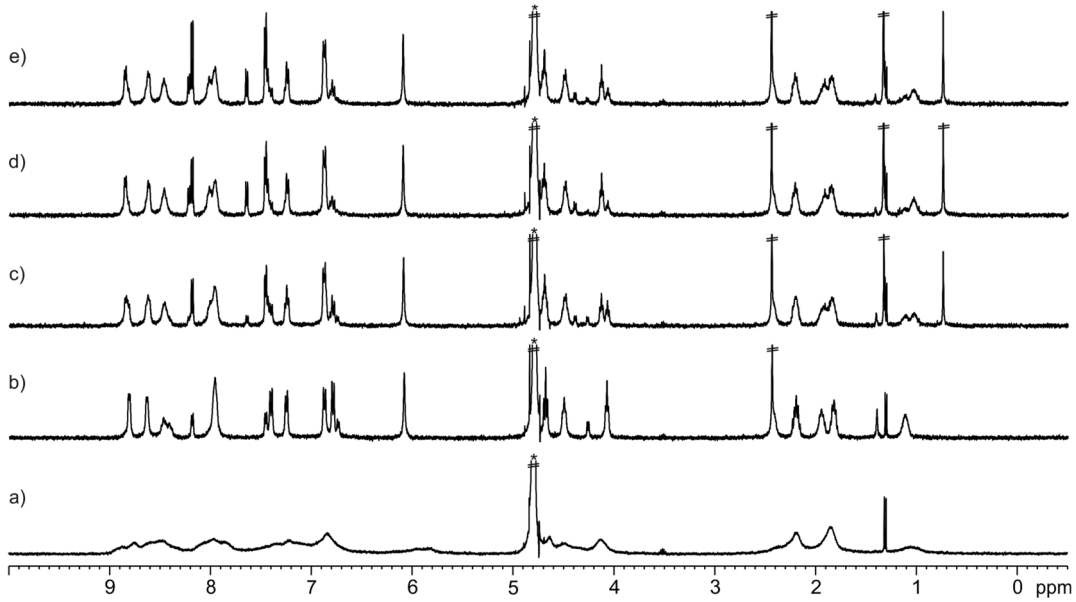

Figure S81. ^{1}H NMR (400 MHz, D_2O, 298 K) spectra of the pair-wise competitive experiment of **6**, **8c** and **8d**: a) **6**; b) **8d** + **6** (2.5:1 molar ratio); c) **8c** + **8d** + **6** (1.2:2.5:1 molar ratio); d) **8c** + **8d** + **6** (2.5:2.5:1 molar ratio) and e) **8c** + **8d** + **6** (2.5:3.9:1 molar ratio). *Solvent residual peak.

Integration of selected proton signals in the spectra of the pair-wise competitive experiments indicated that K_a (**8c**⊂**6**) = 4.5±0.4 x K_a (**8d**⊂**6**).

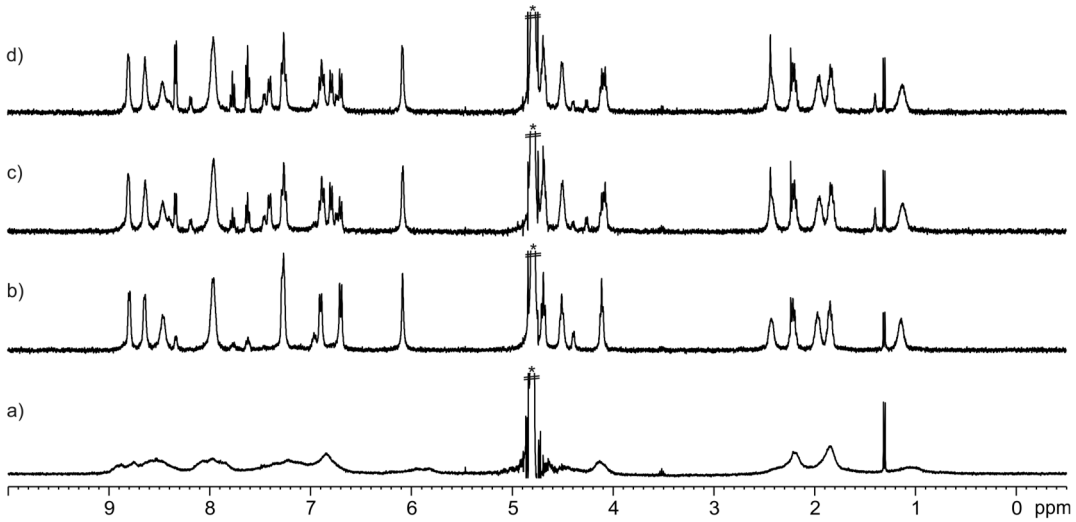

Figure S82. ^{1}H NMR (400 MHz, D_2O, 298 K) spectra of the pair-wise competitive experiment of **6**, **8d** and **8e**: a) **6**; b) **8e** + **6** (1.8:1 molar ratio); c) **8d** + **8e** + **6** (1.2:1.8:1 molar ratio) and d) **8d** + **8e** + **6** (1.2:3.2:1 molar ratio). *Solvent residual peak.

Integration of selected proton signals in the spectra of the pair-wise competitive experiments indicated that K_a (**8d**⊂**6**) = 3.7±0.2 x K_a (**8e**⊂**6**). This result is in line with that obtained from the ITC titration experiments.

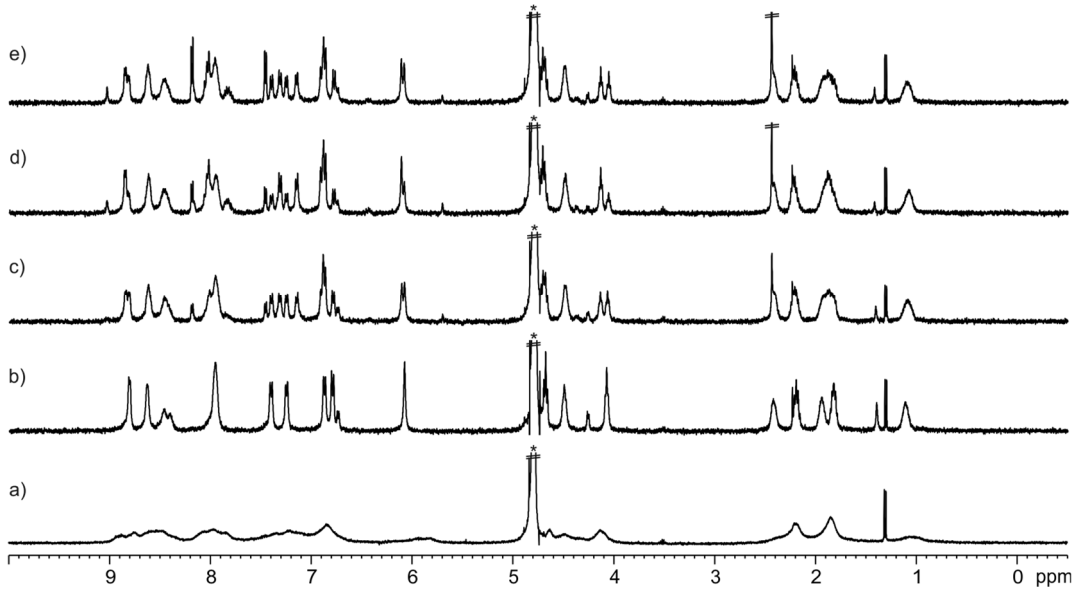

Figure S83. ^{1}H NMR (400 MHz, D_2O, 298 K) spectra of the pair-wise competitive experiment of **6**, **8d** and **8f**: a) **6**; b) **8d** + **6** (1:1 molar ratio); c) **8f** + **8d** + **6** (1:1:1 molar ratio); d) **8f** + **8d** + **6** (2:1:1 molar ratio) and e) **8f** + **8d** + **6** (2:2:1 molar ratio). *Solvent residual peak.

Integration of selected proton signals in the spectra of the pair-wise competitive experiments indicated that K_a (**8f**⊂**6**) = 2.5±0.5 x K_a (**8d**⊂**6**). This result is in line with that obtained from the ITC titration experiments.

9. ITC titration experiments of octa-acid 5 with pyridyl *N*-oxides

ITC experiments were performed in a MicroCal VP-ITC MicroCalorimeter with the VP Viewer 2000 software. Titrations were carried out by adding small aliquots (8-10 μL) of a water solution of the guest into a solution of the host in the same solvent. The concentration of guest solutions was approximately seven to ten times more concentrated than receptor solutions. The association constants and the thermodynamic parameters were obtained from the fit of the titration data to the "one set of sites" binding model implemented in the Microcal ITC Data Analysis module.

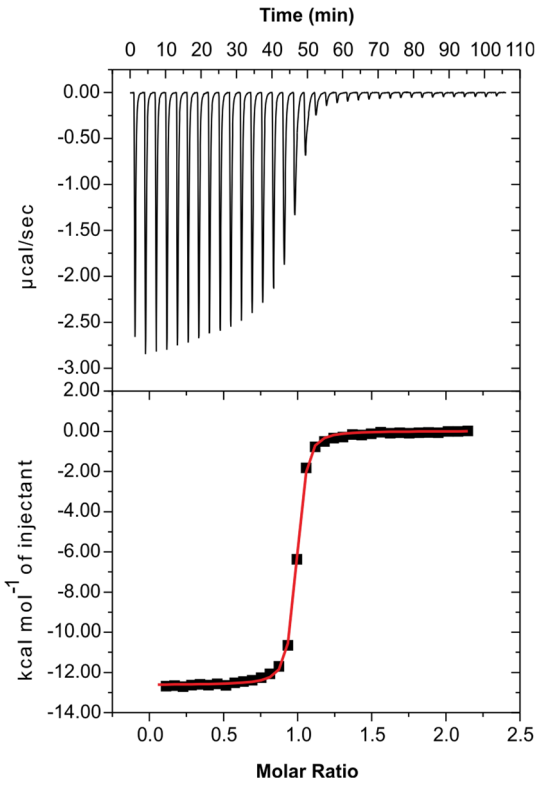

Figure S84. Trace shows raw data for the titration of **8a⊂5** in water at pH ~ 10 (top). Titration was performed at 25ºC. Binding isotherm of the calorimetric titration shown on top (bottom). The enthalpy of binding for each injection is plotted against the molar ratio of guest/host in the cell. The continuous line represents the least-squares-fit of the data to a single-site binding model.

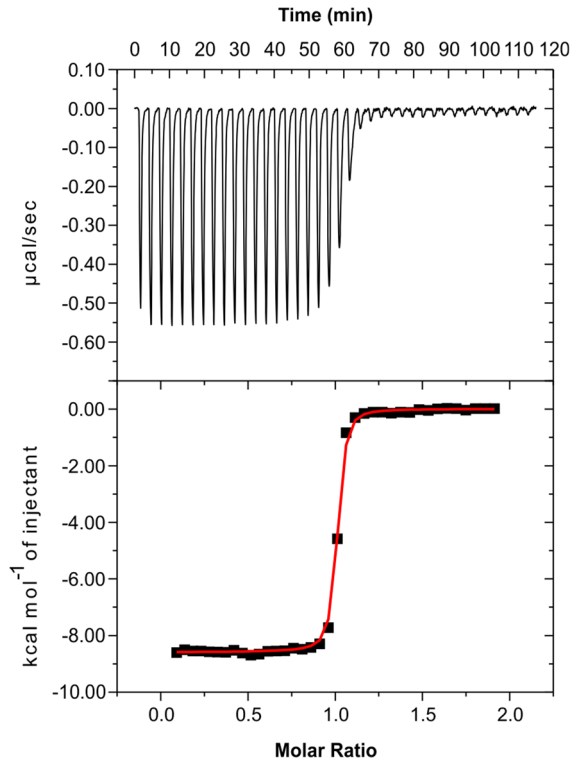

Figure S85. Trace shows raw data for the titration of **8b⊂5** in water at pH ~ 10 (top). Titration was performed at 25ºC. Binding isotherm of the calorimetric titration shown on top (bottom). The enthalpy of binding for each injection is plotted against the molar ratio of guest/host in the cell. The continuous line represents the least-squares-fit of the data to a single-site binding model.

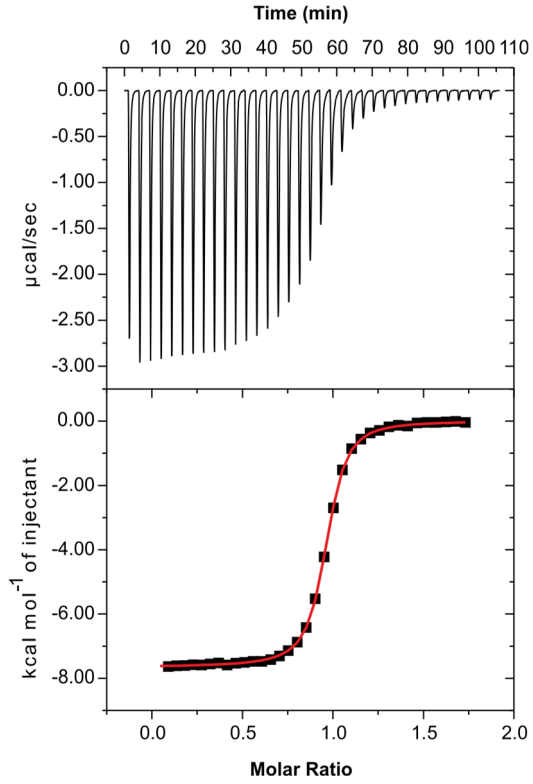

Figure S86. Trace shows raw data for the titration of **8d⊂5** in water at pH ~ 10 (top). Titration was performed at 25ºC. Binding isotherm of the calorimetric titration shown on top (bottom). The enthalpy of binding for each injection is plotted against the molar ratio of guest/host in the cell. The continuous line represents the least-squares-fit of the data to a single-site binding model.

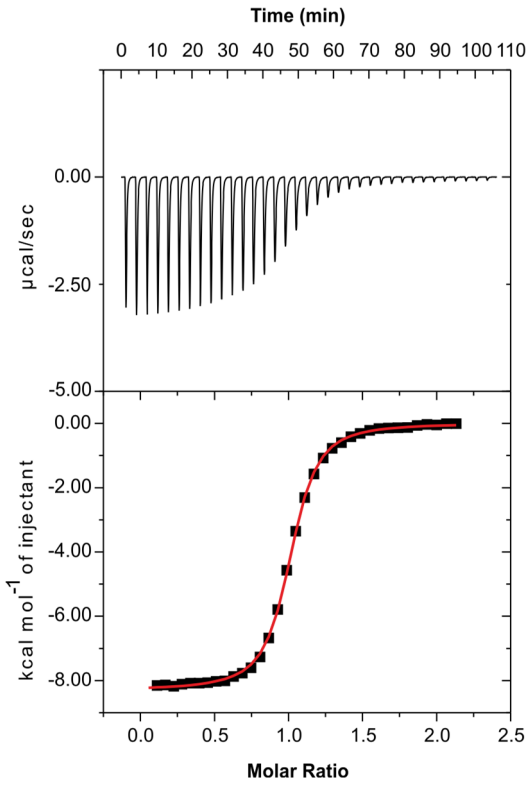

Figure S87. Trace shows raw data for the titration of **8e⊂5** in water at pH ~ 10 (top). Titration was performed at 25ºC. Binding isotherm of the calorimetric titration shown on top (bottom). The enthalpy of binding for each injection is plotted against the molar ratio of guest/host in the cell. The continuous line represents the least-squares-fit of the data to a single-site binding model.

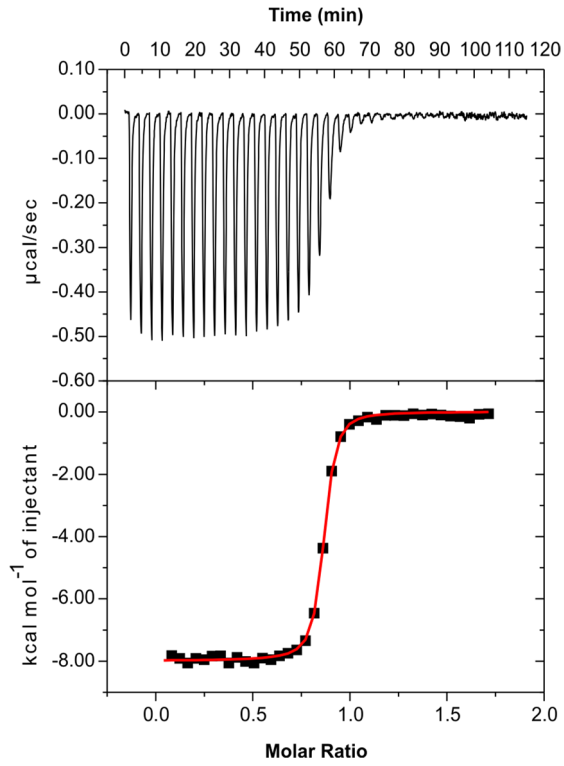

Figure S88. Trace shows raw data for the titration of **8f⊂5** in water at pH ~ 10 (top). Titration was performed at 25ºC. Binding isotherm of the calorimetric titration shown on top (bottom). The enthalpy of binding for each injection is plotted against the molar ratio of guest/host in the cell. The continuous line represents the least-squares-fit of the data to a single-site binding model.

Table S15. Binding constants (K_a, M^{-1}) and thermodynamic parameters (ΔH, $T\Delta S$ and ΔG, kcal·mol^{-1}) determined from the combination of the ITC titration experiments and the pair-wise competitive experiments in water (pD or pH ~ 10) at 298 K. Errors in K_a and ΔG are reported as standard deviations.

Entry	Complex	K_a	ΔH	$T\Delta S$	ΔG
1	**8a**⊂**5**	$>10^7$ [a]	-12.5±0.1 [b]		
		$1.2\pm0.5 \times 10^9$ [c]		-0.1±0.4 [d]	-12.4±0.4 [c]
2	**8b**⊂**5**	$>10^7$ [a]	-8.7±0.1 [b]		
		$1.0\pm0.4 \times 10^8$ [c]		2.2±0.2 [d]	-10.9±0.2 [c]
3	**8c**⊂**5**	$9.1\pm3.0 \times 10^6$ [c]	nd	nd	-9.5±0.2 [c]
4	**8d**⊂**5**	$2.0\pm0.1 \times 10^6$ [b]	-7.7±0.1 [b]	0.9±0.1 [b]	-8.6±0.1 [b]
5	**8e**⊂**5**	$8.6\pm0.5 \times 10^5$ [b]	-8.4±0.1 [b]	-0.3±0.1 [b]	-8.1±0.1 [b]
6	**8f**⊂**5**	$2.2\pm0.2 \times 10^7$ [b]	-7.8±0.2 [b]	2.2±0.2 [b]	-10.0±0.1 [b]

[a] Estimated from ITC experiments; [b] determined by ITC experiments; [c] determined by pair-wise competitive experiments; [d] determined using the thermodynamic constants measured by ITC and pair-wise competitive experiments; nd = not determined.

Concentration of the solutions used in the ITC titration experiments: 1) [**8a**] = 0.70 mM and [**5**] = 0.08 mM; 2) [**8b**] = 0.35 mM and [**5**] = 0.05 mM; 4) [**8d**] = 1.30 mM and [**5**] = 0.15 mM; 5) [**8e**] = 1.30 mM and [**5**] = 0.13 mM and 6) [**8f**] = 0.35 mM and [**5**] = 0.05 mM.

10. ITC titration experiments of octa-pyridinium 6 with pyridyl *N*-oxides

ITC experiments were performed in a MicroCal VP-ITC MicroCalorimeter with the VP Viewer 2000 software. Titrations were carried out by adding small aliquots (8-10 μL) of a water solution of the guest into a solution of the host in the same solvent. The concentration of guest solutions was approximately seven to ten times more concentrated than receptor solutions. The association constants and the thermodynamic parameters were obtained from the fit of the titration data to the "one set of sites" binding model implemented in the Microcal ITC Data Analysis module.

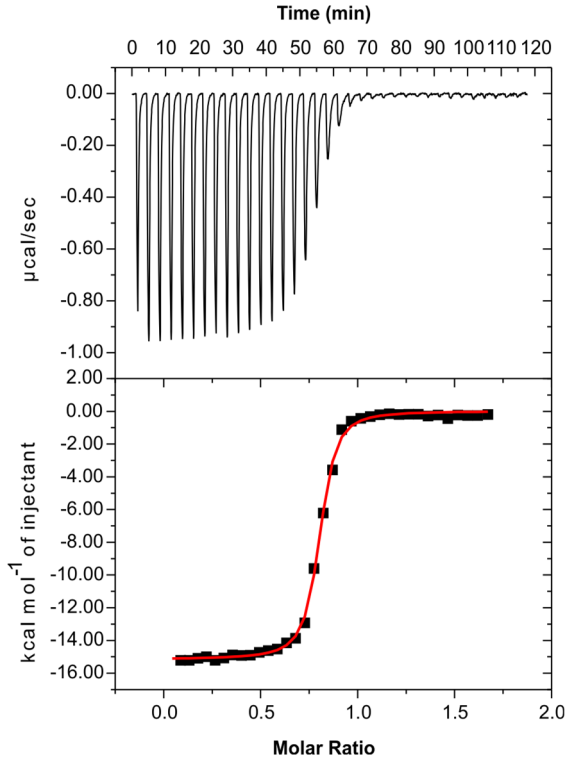

Figure S89. Trace shows raw data for the titration of **8a⊂6** in water (top). Titration was performed at 25ºC. Binding isotherm of the calorimetric titration shown on top (bottom). The enthalpy of binding for each injection is plotted against the molar ratio of guest/host in the cell. The continuous line represents the least-squares-fit of the data to a single-site binding model.

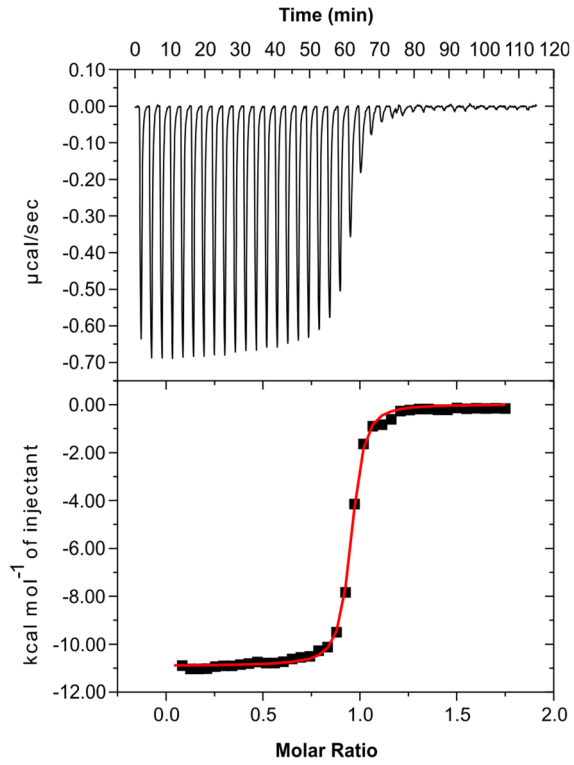

Figure S90. Trace shows raw data for the titration of **8b⊂6** in water (top). Titration was performed at 25ºC. Binding isotherm of the calorimetric titration shown on top (bottom). The enthalpy of binding for each injection is plotted against the molar ratio of guest/host in the cell. The continuous line represents the least-squares-fit of the data to a single-site binding model.

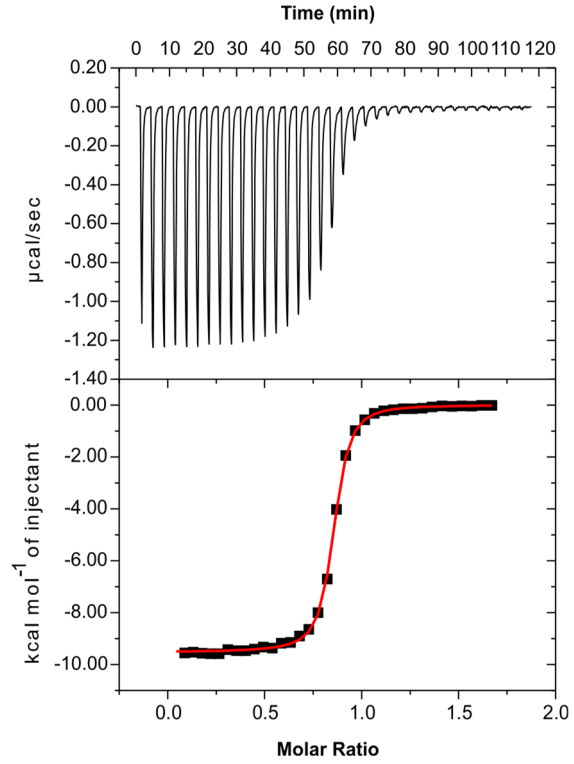

Figure S91. Trace shows raw data for the titration of **8d⊂6** in water (top). Titration was performed at 25ºC. Binding isotherm of the calorimetric titration shown on top (bottom). The enthalpy of binding for each injection is plotted against the molar ratio of guest/host in the cell. The continuous line represents the least-squares-fit of the data to a single-site binding model.

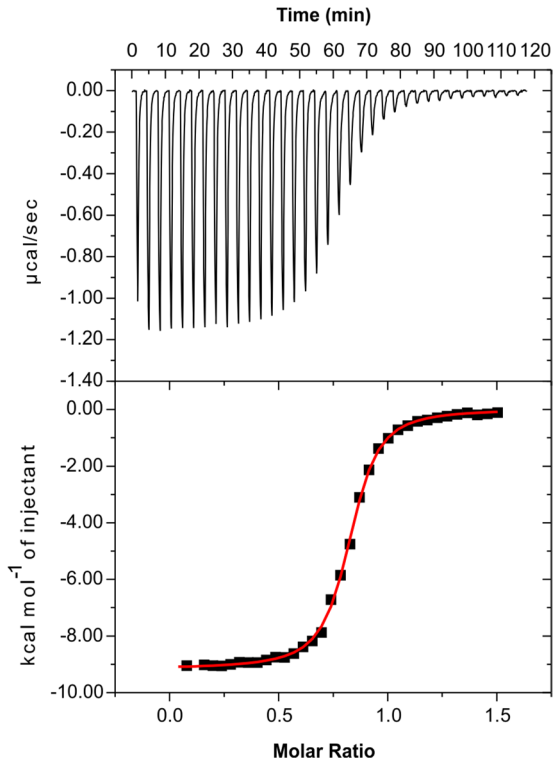

Figure S92. Trace shows raw data for the titration of **8e⊂6** in water (top). Titration was performed at 25ºC. Binding isotherm of the calorimetric titration shown on top (bottom). The enthalpy of binding for each injection is plotted against the molar ratio of guest/host in the cell. The continuous line represents the least-squares-fit of the data to a single-site binding model.

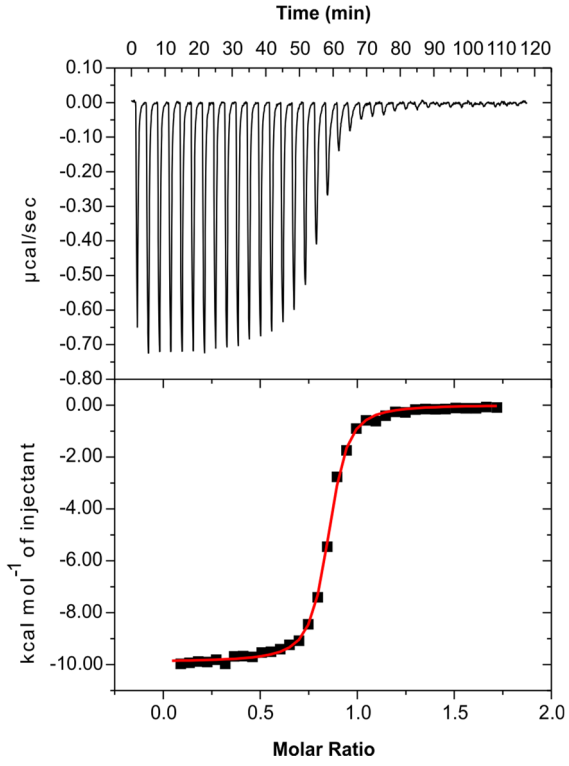

Figure S93. Trace shows raw data for the titration of **8f⊂6** in water (top). Titration was performed at 25ºC. Binding isotherm of the calorimetric titration shown on top (bottom). The enthalpy of binding for each injection is plotted against the molar ratio of guest/host in the cell. The continuous line represents the least-squares-fit of the data to a single-site binding model.

Table S16. Binding constants (K_a, M^{-1}) and thermodynamic parameters (ΔH, $T\Delta S$ and ΔG, $kcal \cdot mol^{-1}$) determined from the combination of the ITC titration experiments and the pair-wise competitive experiments in water at 298 K. Errors in K_a and ΔG are reported as standard deviations.

Entry	Complex	K_a	ΔH	$T\Delta S$	ΔG
1	**8a**⊂**6**	$>10^7$ [a]	-15.1±0.1 [b]		
		$2.6\pm0.6 \times 10^9$ [c]		-2.3±0.1 [d]	-12.8±0.1 [c]
2	**8b**⊂**6**	$>10^7$ [a]	-11.0±0.1 [b]		
		$3.7\pm0.6 \times 10^8$ [c]		0.7±0.1 [d]	-11.7±0.1 [c]
3	**8c**⊂**6**	$3.7\pm0.6 \times 10^7$ [c]	nd	nd	-10.3±0.1 [c]
4	**8d**⊂**6**	$6.1\pm0.1 \times 10^6$ [b]	-9.5±0.1 [b]	-0.3±0.1 [b]	-9.2±0.1 [b]
5	**8e**⊂**6**	$1.9\pm0.1 \times 10^6$ [b]	-9.1±0.1 [b]	-0.5±0.1 [b]	-8.6±0.1 [b]
6	**8f**⊂**6**	$7.1\pm0.2 \times 10^6$ [b]	-10.1±0.2 [b]	-0.8±0.2 [b]	-9.3±0.1 [b]

[a] Estimated from ITC experiments; [b] determined by ITC experiments; [c] determined by pair-wise competitive experiments; [d] determined using the thermodynamic constants measured by ITC and pair-wise competitive experiments; nd = not determined.

Concentration of the solutions: 1) [**8a**] = 0.35 mM and [**6**] = 0.05 mM; 2) [**8b**] = 0.35 mM and [**6**] = 0.05 mM; 4) [**8d**] = 0.70 mM and [**6**] = 0.10 mM; 5) [**8e**] = 0.70 mM and [**6**] = 0.10 mM and 6) [**8f**] = 0.35 mM and [**6**] = 0.05 mM.

11. Relationship between the free energies of binding and the surface area of the non-polar substituents

Table S17. Difference in free energy ($\Delta\Delta G$ = ΔG [(**8a**-**d**)⊂SAE-C[4]P] - ΔG [**8e**⊂SAE-C[4]P], kcal·mol^{-1}) and surface areas (ΔA = A (**8a**-**d**) - A (**8e**), Å^2) of the non-polar *para*-substituent for the complexes of the pyridyl *N*-oxide derivatives with water-soluble SAE-C[4]Ps **5** and **6**.

Guest	A	ΔA	$\Delta\Delta G$ (receptor **5**)	$\Delta\Delta G$ (receptor **6**)
8a	180	71	-4.3±0.4	-4.2±0.1
8b	183	74	-2.8±0.2	-3.1±0.1
8c	170	61	-1.4±0.2	-1.7±0.1
8d	128	19	-0.5±0.1	-0.6±0.1
8e	109	0	0.0±0.1	0.0±0.1

Plot of $\Delta\Delta G$ *versus* ΔA:

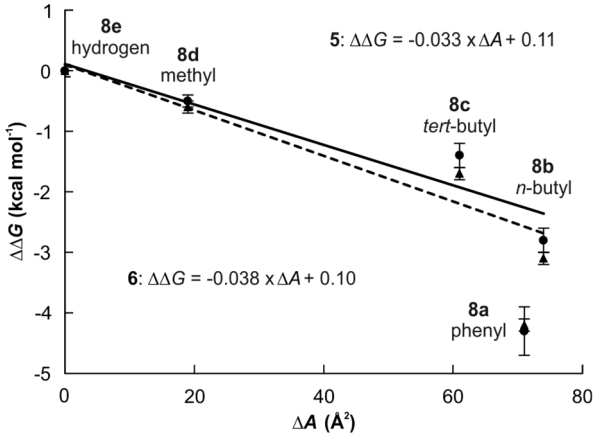

Figure S94. Difference in free energy ($\Delta\Delta G$) *vs.* surface area (ΔA) of the non-polar *para*-substituent for the complexes of the pyridyl *N*-oxide derivatives with water-soluble SAE-C[4]Ps. The data of the complexes of **5** and **6** are shown as circles and triangles, respectively. The linear fits of the data are represented as solid and dashed lines for complexes of **5** and **6**, respectively. Error bars are standard deviations.

12. References

[1] G. R. Fulmer, A. J. M. Miller, N. H. Sherden, H. E. Gottlieb, A. Nudelman, B. M. Stoltz, J. E. Bercaw and K. I. Goldberg, *Organometallics*, 2010, **29**, 2176-2179.

[2] A. Díaz-Moscoso, D. Hernández-Alonso, L. Escobar, F. A. Arroyave and P. Ballester, *Org. Lett.*, 2017, **19**, 226-229.

[3] V. Fiandanese, G. Marchese, V. Martina and L. Ronzini, *Tetrahedron Lett.*, 1984, **25**, 4805-4808.

[4] B. Scheiper, M. Bonnekessel, H. Krause and A. Furstner, *J. Org. Chem.*, 2004, **69**, 3943-3949.

[5] A. Spurg and S. R. Waldvogel, *Eur. J. Org. Chem.*, 2008, 337-342.

[6] Y. He, S. Liu, A. Menon, S. Stanford, E. Oppong, A. M. Gunawan, L. Wu, D. J. Wu, A. M. Barrios, N. Bottini, A. C. B. Cato and Z.-Y. Zhang, *J. Med. Chem.*, 2013, **56**, 4990-5008.

[7] L. Escobar, G. Aragay and P. Ballester, *Chem.--Eur. J.*, 2016, **22**, 13682-13689.

[8] D. A. Lightner, Nicolett.R, G. B. Quistad and E. Irwin, *Org. Mass Spectrom.*, 1970, **4**, 571-585.

[9] S. Duric and C. C. Tzschucke, *Org. Lett.*, 2011, **13**, 2310-2313.

[10] K. Krynicki, C. D. Green and D. W. Sawyer, *Faraday Discuss.*, 1978, **66**, 199-208.